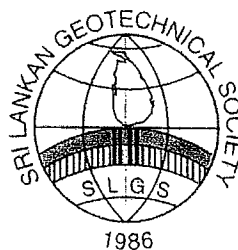


# **GEOTECHNICAL ENGINEERING PROJECT DAY 2016**

A Presentation of Best Geotechnical Engineering  
Undergraduate Projects in  
Sri Lankan Universities

**September 14, 2016  
At CIDA Auditorium**

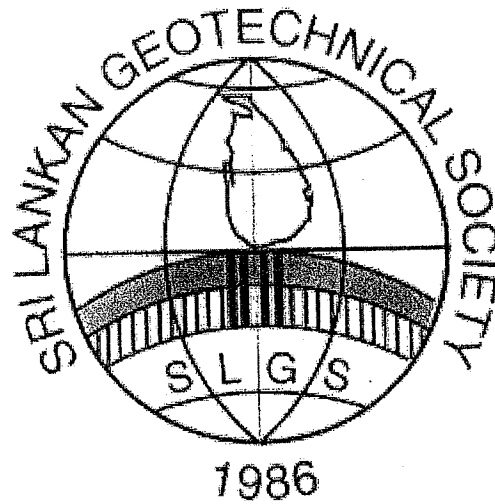
**Organised by the  
SRI LANKAN GEOTECHNICAL SOCIETY**



**SLGS**



**GEOTECHNICAL ENGINEERING  
PROJECT DAY – 2016**





## Message from the President - SLGS

Sri Lankan Geotechnical Society is very happy to stage the Project Day 2016 competition with nine very good quality papers from undergraduates of Sri Lankan Universities who have done projects in the field of geotechnical engineering. It is pleasing to see a good variety of papers with both numerical and experimental studies over the full spectrum of geotechnical engineering.

Participants will get the opportunity to publish their paper in a national conference and present their work to an audience of senior engineers. The best paper and the second paper will receive cash awards and certificates.

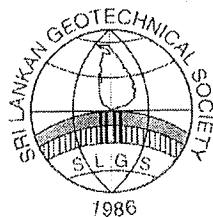
The Project Day competition which started in year 2000 has produced many winners most of whom have proceeded to do higher studies in the field. Many of them have established good carriers in the field of Geotechnical Engineering as both academics and practicing engineers.

I also wish to convey my sincere gratitude to the panel of evaluators; Emeritus Professor B. L. Tennekoon, Mr. K. S. Senanayake and Dr. H. G. P. A. Ratnaweera.

Prof. Athula Kulathilaka  
President - SLGS

## CONTENTS

(1)	<p>Finite Element Analysis of a Deep Excavation Supported by an Anchored Diaphragm Wall</p> <p>H. M. C. N. Rathnayake Department of Civil Engineering, University of Moratuwa, Sri Lanka</p>	1 - 4
(2)	<p>Effect of salinity on consolidation of peat</p> <p>K.H.S.S. De Silva Department of Civil Engineering, University of Moratuwa, Sri Lanka</p>	5 - 8
(3)	<p>Comparison of Stone Column Design Methods</p> <p>W. L. D. H. A. Perera Department of Civil Engineering, University of Moratuwa, Sri Lanka</p>	9 - 12
(4)	<p>Optimization of landfill final cover based on gas exchangeable properties of soil</p> <p>M.H. Samarakoon and E.B.S. Madushan Department of Civil and Environmental Engineering, Faculty of Engineering, University of Ruhuna, Sri Lanka.</p>	13 - 16
(5)	<p>Effect of Rainfall on Slope Failures in Unsaturated Soil</p> <p>A.B.K.A. Lakmali and H.B.P. Raveendra Department of Civil and Environmental Engineering, Faculty of Engineering, University of Ruhuna</p>	17 - 20
(6)	<p>Analysis of Soil-nail Pullout Interaction in Lateritic Soil using Laboratory Models</p> <p>B. L. A. Isaka and B. C. Madushanka Department of Civil and Environmental Engineering, Faculty of Engineering, University of Ruhuna</p>	21 - 24
(7)	<p>Experimental Investigation on Strength and Deformation Characteristics of Crushed Concrete Aggregate</p> <p>R. K. S. R. Ratnayake Department of Civil Engineering, University of Moratuwa, Sri Lanka</p>	25 - 28
(8)	<p>Determination of Age of Municipal Solid Waste through Soil Tests</p> <p>J. Thirojan Department of Civil Engineering, University of Moratuwa, Sri Lanka</p>	29 - 34
(9)	<p>A Study on the Application of Poker Vibrator for Compacting Quarry Dust</p> <p>K.H.S.M. Sampath Department of Civil Engineering, University of Moratuwa, Sri Lanka</p>	35 - 38



# Finite Element Analysis of a Deep Excavation Supported by an Anchored Diaphragm Wall

H.M.C.N. Rathnayake

Department of Civil Engineering, University of Moratuwa, Sri Lanka

**ABSTRACT:** Two zoned excavation, 4m & 11m deep for the construction of ITC Hotel at Galle Face supported by an anchored diaphragm wall is reviewed through this research. This paper presents a back analysis for the excavated zone 1 using computer program PLAXIS based on finite element method & predict the settlement in zone 2 which is expected to excavate. The geotechnical parameters were selected based on the soil investigation report carried out for the purpose of the construction. All soil were modeled using "Mohr Coulomb soil model" and drained analysis were carried out. The lateral movement of the diaphragm wall, settlement of the ground calculated from the FEM analysis were compared with the actual field measurement taken by total station & inclinometers. Finally differences between field measurements and FEM analysis results were discussed and anticipated settlement for the zone 2 wall section was predicted. Some suggestions for the use of FEM model to simulate the deep excavation supported by anchored diaphragm wall are also presented.

## 1 INTRODUCTION

### 1.1 Deep excavation & diaphragm wall

Deep excavations are widely used in urban areas for the purpose of basement for the high rise buildings. Lateral support to the retained soil should be provided in any method. In any type of means for the lateral support it should be capable of withstand the self-weight, retained soil and bear the working load on retain side. Diaphragm walls, sheet piles, soldier piles and lagging, contiguous piles, secant piles are widely used methods. For the construction of basement for the ITC Hotel, Galle Face, excavation was proceed with the diaphragm wall. In this research behavior of this diaphragm wall is reviewed.

Diaphragm wall is constructed using a narrow trench excavated in ground and supported by bentonite mud until the mud is replaced by the reinforced concrete. Normally wall is constructed up to the bed rock to avoid seepage under the wall & anchors are installed at necessary depth as decide by design.

### 1.2 Site condition

Excavation area which consist of sandy soil was divided into two zones. Zone 1 has excavation depth of 4 m while zone 2 has 11 m. existing ground level is about 9 m MSL and GWL was encountered at 5 m MSL. Prior to main excavation site clearance was done up to 5 m MSL.

Diaphragm wall has a thickness of 600 mm & height is about 21 m but it is varied with the bed rock level. Zone 1 is supported by single anchor

level which was installed at an angle of  $15^\circ$  at 3.9 m depth & nearly 1 m spacing. Each anchor was subjected to prestressed force of 40 tons. In zone 2, wall has three anchor levels installed at 3.9, 7.9 & 10.9 m and prestressed by forces of 40, 50 & 60 tons respectively. Angle & spacing of anchors are same as zone 1 excavation.

### 1.3 Literature review

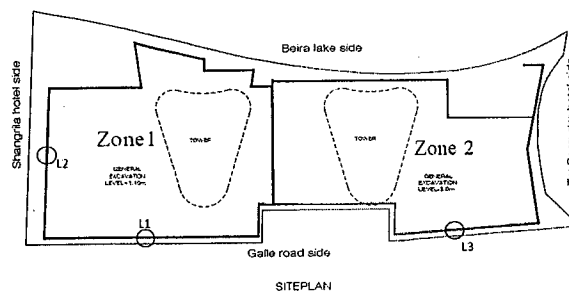


Figure 1. Site plan

Few researches of similar type of problem were carried out by Tan et al. (2001), Likitlersuang et al. (2013), Li et al. (2015). Following facts were observed through above researches.

2D plain strain FEM approach can be adopted. Residual soil can be modeled by hardening soil model, soil stiffness has considerable influence on the wall movement, and the patterns of wall movement depend on the sub soil condition & support system. If soil is predominantly sandy cantilever type wall movement can occur, if soft soil is encountered deep inward movement is more likely to be encountered.

However there was no research is conducted in Sri Lanka to understand behavior of a diaphragm wall (D-wall).

## 2 OBJECTIVES

Objective of this research are

- i. Comparison of the field monitoring records of D-wall with the FEM result.
- ii. Predict the lateral deformation of D-wall in zone 2
- iii. Check the suitability of FEM to predict the deformation of deep excavation supported by anchored D-wall

## 3 SUBSURFACE CONDITION

Subsurface investigation was carried out by advancing 19 boreholes using wash boring method within the excavation area. SPT test was carried out in the bore holes. Subsurface is mainly consist with sandy soil. But in five bore holes stiff clay layer was identified. Since no information available for the geotechnical parameters in the soil investigation report.  $E$ ,  $F'$ ,  $C'$  were estimated using empirical correlations.

Generally soil stratification thickness was observed as follows. Top soil layer of 1.5 m thickness, loose sand layer of 1.5 m thickness, medium dense to very dense sand layer of 15 m thickness and completely weathered rock layer of 7 m thickness. After that bed rock was encountered. Average depth to bed rock was about 24 m. since site was excavated up to reduced level of 5 m MSL, top soil & loose sand layers were not observed. Therefore their properties were not considered. Summary of geotechnical parameters used for further calculations are listed below.

Table 1. Geotechnical parameters

	SPT N	$\gamma_{sat}$ kN/m <sup>3</sup>	E kPa	C' kPa	F'
Medium dense to very dense sand	40	21	50,000	1	38
Stiff silty clay	15	16	15,000	8	26
Completely weathered rock	30	21	40,000	10	38

$\gamma_{sat}$  - saturated density of soil, E - modulus of elasticity

C' - cohesion, F' - friction angle

## 4 SIMULATION OF THE BEHAVIOUR OF THE D-WALL

Three locations in the D-wall was considered for the analysis. Availability of nearby deformation

monitoring point & existence of considerable straight length in wall was considered in the selection of locations. Two locations was situated in zone 1 while remaining one was in the zone 2. Refer to Figure 1 for the locations.

Numerical analysis was carried out in plane strain and 15-nodes triangular elements. Model size should have to be sufficiently large in order to maintain the accuracy of results. Therefore length was selected as two times the height of D-wall plus additional 15m for excavation side. Height was taken as equal to the D-wall height. Two vertical sides kept in roller boundary conditions, while the bottom was fixed. Medium coarse mesh was used. Ground water table considered as coincide with surface preparation level. All soil types were modeled using Mohr-coulomb model and D-wall simulated in linear elastic model. Bed rock was simulated as fixed boundary. Free length of pre stressed anchor is simulated as node to node element while fixed length was idealized as grout body which has only axial stiffness. Actual properties of grouted area was not been able to gather. Therefore in the simulation it was ensured that movement of grout body i.e. fixed length is extremely minimal. The factor  $R_{inter}$  was used in order to reduce the strength properties of the interface elements with respect to the surrounding soil. In this research 0.7 was used. The key input soil parameters are listed in table 1.

Table 2. Location details

Location	zone 1		zone 2
	L1	L2	L3
excavation depth (m)	4	4	11
D-wall height (m)	21	24	18
Anchors level depth (m) & force(ton)	3.9-40	3.9-40	3.9-40 7.9 - 50 10.9 - 60
Soil profile: layer & thickness (m)	MDVDS-15	MDVDS-14	MDVDS-14
	CWR-6	SSC-3	CWR-4
		CWR-7	

MDVDS - medium dense to very dense sand

SSC - stiff silty clay

CWR - completely weathered rock

All depth are measured form reduced ground level (5 m MSL)

Refer figure 1 for the locations

Excavation up to 5m MSL is not considered as a construction stage. Since it was already done prior to the construction of the wall. Therefore 70 kN/m<sup>2</sup> surcharge was applied on the retained side about 5 m away from D-wall. Furthermore from 1.5 m beyond wall up to 5 m nominal surcharge load of



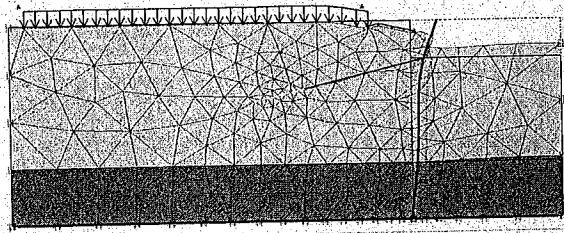
Excavation up to 5m MSL is not considered as a construction stage. Since it was already done prior to the construction of the wall. Therefore 70 kN/m<sup>2</sup> surcharge was applied on the retained side about 5 m away from D-wall. Furthermore from 1.5 m beyond wall up to 5 m nominal surcharge load of 10 kN/m<sup>2</sup> applied. Construction sequence was simulated as follows.

For L1 & L2, first installation of D-wall & application of surcharge load. Then bulk excavation up to 4 m followed by dewatering. After that pre-stressing was conducted.

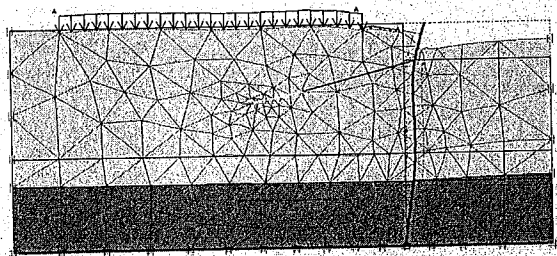
For the location 3, installation of D-wall & application of surcharge load. Bulk excavation up to 4 m depth, pre-stressing with 40 tons force, second bulk excavation up to 8 m, pre-stressing with 50 tons force, final excavation up to 11 m depth followed by pre-stressing with 60 tons force. Dewatering process was continued in steady state condition while the excavation continues.

### 5 RESULTS

Back analyzed results of this research paper presents the absolute lateral displacement of the D-wall and the settlement of the retained ground behind the wall.



Location 1



Location 2

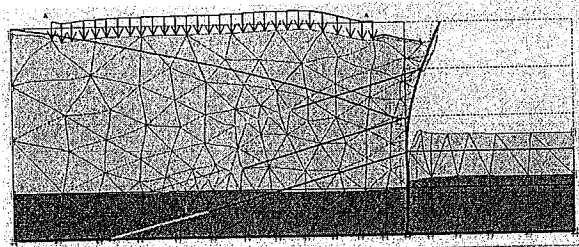


Figure 2. Deformed mesh of FE model

But field measurements taken from the inclinometer reading has some errors due to technical issues like non verticality of inclinometer shaft. Therefore deflected profile was not able to compare with above field monitoring record. As such tilt monitoring record taken from the top of the wall measured precisely with total station was used.

Figure 3 shows the lateral deformation of the wall after complete excavation and anchoring. L1 graph shows the cantilever shape because soil is

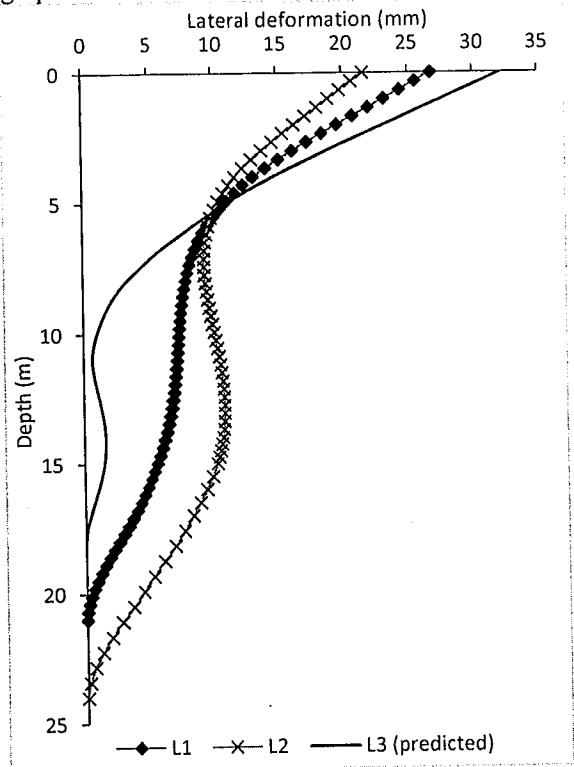


Figure 3. Lateral deformation of wall vs depth (FEM analysis)

predominantly sand. local sagging behavior at a depth of 6 m is caused by the pre-stressed applied at 3.9 m level. L2 graph shows the deep inward movement because the clay layer present at 14 m depth. In L3 graph portion above the 10 m shows a cantilever behavior while bottom part has low deformation this is mainly cause of three level of anchors. These deflected shape of the D-wall was revealed through the field observations of inclinometer readings.

Table 3. FEM analysis result & actual field monitored readings of the D-wall

lateral deformation(mm)		Settlement (mm)	
FEM	Actual	FEM	Actual

(Note: Lateral deformation were taken at the top of the wall, Settlement implied the ground settlement just behind the wall. L3 is intended to excavate hence field observation are not available)

As per details of table 3. There is approximate match between the FE model results vs the field monitored records. In location L1 FE has slightly under estimated while in location L2 it has been over estimated. When consider about location L2 it is closer to the corner of the D-wall that corner effect cause the reduction of lateral deformation. Propagation of ground settlement is also an important aspect of a deep excavation. FE model has given a significant ground settlement up to 10 m from wall for location L1&L2. Field monitored record for the ground settlements are inadequate therefore it was unable to construction a comparison of FEM vs actual data perpendicular to the D-wall.

Even though field monitoring record were precisely taken there are some influence while drilling holes for the pre-stressed anchors. Due to the void created, local ground settlement can occur. Sometimes local sub soil profile may change rather than assumed profile by interpolation of adjacent bore-hole data. There was a capping beam to tie up all D-wall panels. It has great influence on the reduction of lateral movement of wall but in the FE model that behavior can't be simulated. In this research, geotechnical data was interpreted from the SPT N values using empirical correlations. But actual parameters may differ from the predicted ones. For all soil models, Mohr-coulomb model was used. Due to the lack of advanced properties of the soil it was unable to perform the analysis comparing different soil models.

## 6 CONCLUSION

In conclusion, it can be stated that the displacement patterns of the wall obtained from FEM analyses are within the acceptable limits. Except the lateral deformation at location L2, in all other cases predicted values and actual monitored values have a good and reasonable match. Therefore it is evident that sandy soil can be properly modelled using Mohr coulomb soil model for the deep excavation supported by anchored D-wall. The large deviation of lateral deformation of monitored and calculated values at L2 might cause the local variation of subsurface as describe in the earlier chapter.

Furthermore this research has verified that pattern of wall movement is cantilever when subsurface is consist with sandy soil. When soft soil layer is encountered wall shows a bulge behavior at the level of soft soil.

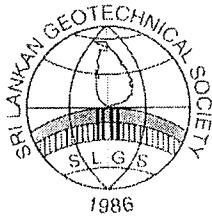
It is also observed that, ground settlement for deep excavation in sandy soils can extend up to a distance of 2-3 times the depth of excavation. The percentage of maximum lateral deformation of the D-wall which is supported by single anchor level installed at bottom is about 0.6% and D-wall supported by multilevel of anchor is about 0.3%.

## ACKNOWLEDGMENTS

Department of Civil Engineering, University of Moratuwa and Project staff ITC Hotel project-Galle Face, Access Engineering PLC are gratefully acknowledged for their support.

## REFERENCES

- Li Q., Wang W.D., XuZ.H., 2015 Design and Behavior of A Deep Excavation Adjacent to Existing Buildings and Tunnels, International conference on geotechnical engineering, Colombo, pp 455-458
- Likitlersuang, S., Surarak, C., Wanatowski, D., Oh, E., and Balasubramaniam, A., (2013), Finite element analysis of a deep excavation: A case study from the Bangkok MRT, Journal of Soils and Foundations, The Japanese Geotechnical Society, 53(5):756-773
- Tan, Y.C., Liew, S.S., Gue, S.S., And Taha, M.R., 2001 A Numerical Analysis of Anchored Diaphragm Walls for a Deep Basement in Kuala Lumpur, Malaysia, 14<sup>th</sup> Southeast Asian Geotechnical Conference, Hong Kong,
- Tutorial manual, PLAXIS version 8



# Effect of Salinity on Consolidation of Peat

K.H.S.S. De Silva

*Department of Civil Engineering, University of Moratuwa, Sri Lanka*

**ABSTRACT:** Peat is a problematic geotechnical material, which could cause large settlements when subjected to loading because of the consolidation effect. Other than the well known factors affecting consolidation of peat, according to Zhang and O'Kelly (2013) addition of salt grains also improves the primary consolidation rate of peat specimens. In this research, the impact of salinity of water for the rate of consolidation was analyzed. The samples were mixed prior to and after addition of salt to achieve identical samples. Kaolin clay samples were used as a control specimen and those samples had no considerable effect on consolidation rate with the addition of salt grains. It was found that under similar conditions of one dimensional loading, consolidation rate of peat can be increased with the addition of salt. For quantitative analysis further experiments are required.

## 1 INTRODUCTION

### 1.1 Consolidation of peat

Peat is a problematic geotechnical material, which causes large settlements when subjected to loading. It consists of decayed organic matter and therefore the characteristics are highly different from ordinary soils. It has an extremely high water content, low shear strength and high compressibility. (O'Kelly, 2009) The permeability is also very high in peat and it has a higher secondary consolidation compared to other clayey soils.

### 1.2 Factors affecting consolidation of peat

Compressibility or consolidation of a soft soil depends on the structure and fabric, stress path, temperature, and the rate of loading. (Lerueil, 1996) That means the strain rate can be expressed as a function of stress, temperature and total strain. (Stolle, D.F.E., 1999) It is hard to express the actual relationship of these parameters with consolidation and material parameters in a laboratory. However the effect of above mentioned factors on compressibility of a soil is well recognized. (Crawford, 1965)

According to the Terzaghi's theory of consolidation, the time for primary consolidation is proportional to  $H^2$ , where  $H$  is the drainage length of the soil under consolidation. However interpreting on field soil behavior from laboratory experiments on consolidation is complicated when viscosity of the soil structure is taken into account. (Joseph, 2014).

Other than these well known factors, according to Zhang and O'Kelly (2013) addition of salt grains also improves the primary consolidation rate of peat specimens. They say that more than one third of the salt additives were removed from the treated peat by the way of expelled pore water and

because of this the amount of creep or secondary consolidation was also reduced. But due to possible environmental and groundwater pollution, using this method is problematic and they suggest that further researches should be done on suitable additives.

Since the composition of peat is organic mostly, there can be reactions with chemical elements and even the composition can be changed in peat. Then compressibility characteristics of peat can also be varied with the different elements in water. Hence consolidation rate of peat may change with the quality of water the peat is saturated.

### 1.3 Salinity

Salinity is the measure of all the salts dissolved in water and it is usually measured in parts per thousand (ppt) or as a percentage of weight, when it comes to water quality. The average ocean salinity is 35ppt and the average river water salinity is 0.5 ppt or less.

In this research the consolidation rate of peat is experimented with salinity or in other words with addition of salt.

## 2 METHODOLOGY

As mentioned earlier, peat has very high water content which leads to higher settlements when dissipated while consolidation process. Salt grains are consisting of Na cations and Cl anions. When they are added in to peat, this ionization of salt grains induces the movement of nearby pore water towards them. Dissolving salt grains also release a high ion concentration water layer around them, producing electrostatic potential and concentration

potential fields that can attract counter ions in the microscope water. (O’Kelly, 2015)

Then the water can easily be removed with loading, with the help of the effect of these ions. Hence the coefficient of permeability is increased and so as the rate of consolidation.

For the process sodium chloride salt was selected to accelerate consolidation since sodium chloride solution has neutral pH. Increases in pH values of the pore water in peat are likely to cause an increase in the rate of decomposition of constituent organic matter. (Pichan and O’Kelly, 2012, 2013).

In this research also sodium chloride salt was used for experiments.

### 3 EXPERIMENTS

#### 3.1 Materials

Laboratory experiments were performed on saturated peat material and saturated kaolin clay material. Kaolin clay samples were used as the control experiment. Peat material was subjected to wet sieve analysis, hydrometer test, Atterberg limit test, Organic content test and specific density test in order to find the properties of the sample and they are shown in Table 1 and Figure 1.

Table 1. Material properties of peat

Property	Value
Sulphate content (%)	24.54
Chloride content (%)	0.00284
Water content (%)	185
Organic content (%)	31.57
Specific gravity	2.2

Oedometer test was carried out for the peat sample and kaolin clay sample under similar conditions. Hereafter the sample sets will be identified as P sample and K sample respectively.

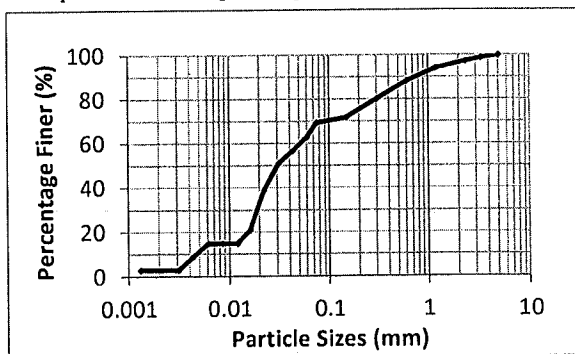


Figure 1. Grading curve of peat sample

#### 3.2 Specimen preparation

Preparation of sample sets with identical conditions (P and K) was done as below.

First sufficient amount from soil was selected and then the harder particles such as stones, decayed tree particles, etc. were removed manually from it. Then the sample was mixed well, for five minutes and was kept for air drying for three days. After that the air dried sample was divided into 5 equal parts, each was 450g in weight. The salt amount added was defined as 2%, 4%, 8% and 16% of weight of initial sample, for the varying concentration of salinity, while keeping all other parameters same and constant. One was kept in its original condition without adding salt. To prepare the oedometer samples following procedure was followed for each sample.

First the soil sample was mixed with required amount of salt. Since the water content the soil wasn't sufficient for mixing, 11 ml of amount of distilled water was also mixed. This was followed by four minutes of mechanical mixing. After that the soil samples were carefully prepared in to pans, avoiding formation of air bubbles inside the sample. Then it was covered with a wetted filter paper to protect moisture loss and then wrapped in polythene cover to assure no moisture would be lost. Then the sample was kept for two days. After two days the samples were used to prepare 50 mm diameter oedometer samples.

K samples were prepared with same procedure.

#### 3.3 Experimental programme

The sample sets P and K were submerged with distilled water in order to avoid additional salinity concentration changes due to water addition for submerging. They were kept submerged for one day before the oedometer tests were conducted.

Oedometer tests were carried out starting from 5 kN/m<sup>2</sup> to 40 kN/m<sup>2</sup> in loading stages. Unloading was carried out in two stages. Then the results were recorded as per the standards (BS 1377) of the oedometer test.

Organic content was found as per the standards of ASTM D 2974, in P sample set and the oedometer samples were used for that after the consolidation test procedure.

### 4 TEST RESULTS AND ANALYSIS

#### 4.1 Test results of oedometer test

The settlement vs. time taken for settlement graphs of sample sets P, K are shown in Figures 2 and 3, respectively.

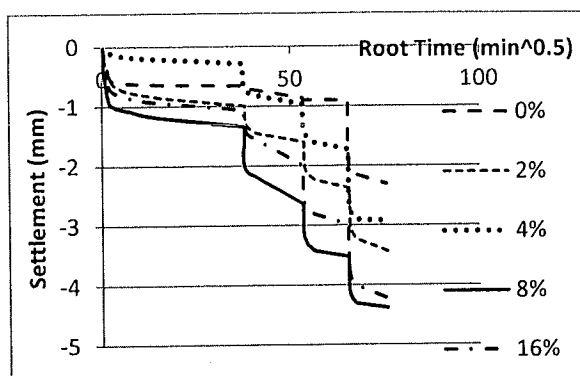


Figure 2. Consolidation test results of sample set P

Figure 3. Consolidation test results of sample set K

Coefficient of consolidation  $c_v$  from square root time method, Coefficient of Volume Compressibility  $m_v$ , Compression index  $c_c$  and Secondary compression index  $c_\alpha$  of above sample sets were determined for each sample for each loading stage.

Results of sample set P are shown in Table 2, Table 3 and Table 4.

Table 2. Coefficient of Consolidation  $c_v$  ( $m^2/year$ )

Sample	Salt added	Loading stages			
		0-5 kPa	5-10 kPa	10-20 kPa	20-40 kPa
1	0%	6.90	42.65	66.51	11.14
2	2%	9.66	14.21	27.38	1.49
3	4%	10.99	9.62	10.2	4.89
4	8%	18.50	27.00	9.27	5.66
5	16%	13.03	17.88	16.97	8.92

Table 3. Coefficient of Volume Compressibility  $m_v$  ( $m^2/kN \times 10^{-3}$ )

Sample	Salt added	Loading stages			
		0-5 kPa	5-10 kPa	10-20 kPa	20-40 kPa
1	0%	6.58	2.19	2.09	3.65
2	2%	9.95	6.41	4.21	2.99
3	4%	2.82	6.94	4.02	3.25
4	8%	13.40	13.90	5.08	2.60
5	16%	10.65	9.88	5.46	3.64

Table 4. Compression index  $c_c$ 

Sample	1	2	3	4	5
Salt added	0%	2%	4%	8%	16%
$c_c$	0.96	0.63	0.58	0.62	0.40

Table 5. Secondary compression index  $c_\alpha \times 10^{-3}$ 

Sample	Salt added	Loading stages			
		0-5 kPa	5-10 kPa	10-20 kPa	20-40 kPa
1	0%	6.102	-	-	7.068
2	2%	-	-	-	-
3	4%	-	-	-	4.662
4	8%	-	-	-	-
5	16%	18.298	18.893	-	-

Results of sample set K are shown in Tables 6, 7, 8 and 9.

Table 6. Coefficient of Consolidation  $c_v$  ( $m^2/year$ )

Sample	Salt added	Loading stages			
		0-5 kPa	5-10 kPa	10-20 kPa	20-40 kPa
1	2%	1.70	1.15	1.98	2.41
2	4%	0.91	1.12	1.75	2.97
3	8%	1.40	1.78	3.82	1.48
4	16%	1.43	19.2	19.12	2.56

Table 7. Coefficient of Volume Compressibility  $m_v$  ( $m^2/kN \times 10^{-3}$ )

Sample	Salt added	Loading stages			
		0-5 kPa	5-10 kPa	10-20 kPa	20-40 kPa
1	2%	9.70	4.78	3.64	2.07
2	4%	6.10	6.50	4.23	2.37
3	8%	11.64	5.33	4.68	2.98
4	16%	5.40	8.43	4.13	2.47

Table 8. Secondary compression index  $c_\alpha \times 10^{-3}$ 

Sample	Salt added	Loading stages			
		0-5 kPa	5-10 kPa	10-20 kPa	20-40 kPa
1	2%	3.269	4.557	5.094	6.469
2	4%	4.844	3.001	7.170	9.949
3	8%	4.262	5.045	7.614	6.939
4	16%	0.468	-	-	1.614

Table 9. Compression index  $c_c$ 

Sample	1	2	3	4
Salt added	2%	4%	8%	16%
$c_c$	0.31	0.50	0.42	0.39

Table 2 and 6 describes the impact of addition of salt on coefficient of consolidation. With the results it can be clearly seen that the addition of salt has not created any considerable impact in K (kaolin clay) sample while there is a considerable impact in P (peat) sample. Also, the addition of salt has increased the consolidation rate. Though the

impact can't be confirmed since sample 4 (8% salt added) sample has higher consolidation rate than sample 5 (16% salt added) sample, it can be only concluded that the impact on coefficient of consolidation seems to be increasing with the addition of salt in peat samples.

Table 3 and 7 describes the impact of addition of salt on volume compressibility. Both samples, it has been reduced with increase of loading; hence the results can't be used to conclude the effect on  $m_v$  of peat evidently. Table 4, 5 and 6, 7 describes the impact of addition of salt on secondary compression and compression index. It can be clearly seen that  $c_c$  has been decreased with the increasing of the salt amount added to the samples. Here also there can't be seen an identifiable alteration in sample set K and sample set P, since both show this impact. However the compression index  $c_c$  values are higher in sample set P than sample set K. Therefore these comparisons confirm the effect of salinity on consolidation is higher in peaty soil types while it has a low impact in non-organic soils like kaolin clay.

Furthermore, Figure 2 shows that the creep effect is also increased compared to Figure 3, with the addition of salt. That means the creep consolidation in peat samples is also affected by the salt addition, since kaolin clay sample doesn't show any creep consolidation.

Calculated sulfate, chloride and organic contents of five samples of sample set P are shown in Table 6 to identify the end condition of samples. It can be seen that the sulfate condition is same in all samples but the chloride content has increased with addition of salt, which should be. Also the organic content of all samples are nearly same and that proves the 5 samples are identical in to greater extent.

Table.5. Chloride, Sulphate and organic contents of sample set P

Sample	Salt added by weight	Sulphate content (%)	Chloride content (%)	Organic content (%)
1	0%	0.64	0.02	39.72
2	2%	0.65	0.44	41.83
3	4%	0.65	0.62	41.50
4	8%	0.55	1.00	44.10
5	16%	0.58	1.69	47.00

## 5 SUMMARY AND CONCLUSION

Under similar conditions of one dimensional loading, consolidation rate of peat can be increased with the addition of salt grains. That means the coefficient of permeability also change with addition of salt grains compared to the original condition. Since the secondary consolidation is higher than

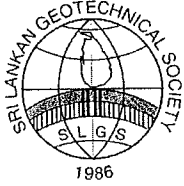
normal, creep consolidation effect can be expected to be minimized since higher settlements have occurred at the beginning. However, quantitative analysis can't be done with this experiments and further research should be done in order to find a measurable impact.

## ACKNOWLEDGMENTS

Dr. U.P. Nawagamuwa is greatly acknowledged for the guidance and Prof. S.A.S. Kulathilake also is greatly acknowledged for the immense guidance and support. Laboratory staff members in Environmental and Soil Mechanics Laboratories are also acknowledged for the support given in conducting experiments

## REFERENCES

- Crawford, C.B. (1965). The resistance of soil structure to consolidation. *Canadian Geotechnical Journal*, 2, 90-97
- Joseph, P.G. (2014). Viscosity and secondary consolidation in one-dimensional loading. *Geotechnical Research*, 1(3), 90-98. doi:10.1680/gr.14.00008
- Ladd, D.C., Foott, R., Ishihara, K., Schlosser, F., & Poulos, H.G. (1977). Stress deformation and strength characteristics. *Proceedings of the 9<sup>th</sup> International Conference on Soil Mechanics and Foundation Engineering*, Tokyo, 2, 421-494
- Leroueil, S. (1996). Compressibility of clay: fundamental and practical aspects. *Journal of Geotechnical Engineering*, ASCE, 122, 534-543
- Leroueil, S. (2006). The isotache approach-where are we 50 years after its development by Professor Suklje. *Professor Suklje's Memorial Lecture, XIII Danube-European Geotechnical Engineering Conference*, Ljubljana, Slovenia. *Slovenian Geotechnical Society*, Ljubljana. 55-58
- O'Kelly B.C. (2009). Development of large consolidometer apparatus for testing peat and other highly organic soils, *SUO-Miras and Peat* 60(1-2):23-26
- Pichan, S.P. and O'Kelly, B.C. (2013). Stimulated decomposition in peat for engineering applications, *Proceedings of the Institution of Civil Engineers – Ground Improvement* 166(3):168-176
- Stolle, D.F.E., Vermeer, P.A. & Bonnier P.G. (1999). A consolidation model for creeping clay *Canadian Geotechnical Journal*, 36, 754-759
- Zhang, L., & O'Kelly, B.C. (2013). Effect of salt grain additions on fibrous peat consolidation. *Ground Improvement*, 168(G/1), 14-21
- Zhang, L. and O'Kelly, B.C. (2015). *Proceedings of the Institution of Civil Engineers – Ground Improvement* 168:14-21.



# Comparison of Stone Column Design Methods

W. L. D. H. A. Perera

*Department of Civil Engineering, University of Moratuwa, Sri Lanka*

**ABSTRACT:** Use of stone columns is a ground improvement technique that can be applied when high embankments are to be constructed on thick layers of soft soils. Stone columns installed in an appropriate pattern, reinforce the soft soil enhancing the shear strength and reducing the settlements. There are several methods for the analysis and design of stone columns. These designs come up with a factor of safety, which cannot be verified in the field. Comparison of Factor of Safety computed with different approaches will be useful in optimizing the design procedures. Designs done with limit equilibrium approach and finite element approach are compared in this research. GEOSLOPE - SLOPE/W software was used for the limit equilibrium approach and PLAXIS 2D software was used for the finite element analysis.

## 1. INTRODUCTION

Due to the unavailability of lands with good sub soil conditions Engineers are compelled to use lands underlain with soft sub soil conditions for infrastructure development projects. In order to avoid shear failures during construction and limit settlements during service, different ground improvement techniques will have to be used. Use of stone columns is one such technique where the soft ground is reinforced by installation of granular columns of high strength and stiffness over a designed grid pattern. The diameter of the column and the spacing are the major design parameters.

Stone columns are extensively used to improve the bearing capacity and possibility of shear failure during construction. It also reduces the settlement of structures built on them. Furthermore, stone columns, accelerate the consolidation and also reduce liquefaction potential of soils.

## 2. STONE COLUMN DESIGN CONCEPTS

Stone columns can carry very high loads since columns are ductile (Mani and Nigee, 2013) and construction can be started soon, since no waiting period is required after installation. Stone columns will carry a greater share of the load applied and stress concentration effect is one of the very important factors in designing of stone columns. Stone columns cannot be used to improve very sensitive clay soils (sensitivity > 4) or very soft clays (Mani and Nigee 2013). Stone columns can

fail by bulging (especially in very soft clays), bending, punching or shearing. Bulging is significant in long columns whereas punching is prominent in shorter columns (McKelvey, Sivakumar, Bell and Graham, 2004).

## 3. METHODOLOGY

In this research stone column designs of similar configuration were done with two alternate approaches; the limit equilibrium approach and the finite element approach. Several variations were adopted within each approach. The behavior of soft clay was modeled under conditions of; drained, undrained and coupled consolidation in the finite element approach, which is more comprehensive and tedious to apply. With much simpler limit equilibrium approach different simplifying assumptions were made.

## 4. MODEL PREPARATION AND PARAMETERS

In both approaches, the stone columns installed in a grid pattern are represented in strips for the plane strain idealization. Several different methods are available within the limit equilibrium approach namely; average shear strength method (considering subsoil as one uniform material without strips), without considering stress concentration on stone column strips and considering stress concentration on stone column strips. The stress concentration effect is used in computing average parameters.

In the finite element approach construction process can be simulated assigning appropriate material

characteristics without making any prior assumptions on stress distribution. PLAXIS 2D was used for the analysis and discretized continuum models were used under plain strain conditions. Drained and undrained soil parameters used for the analysis are summarized in the Table 1. The model types prepared are presented in the Table 2. The model is illustrated in the Fig. 1.

Table 1. Soft soil parameters

Soft Soil Property	Value
$\gamma_{sat}$	15 kN/m <sup>3</sup>
$\gamma_{unsat}$	13 kN/m <sup>3</sup>
$c_p$	10 kN/m <sup>2</sup>
$c$	0.1 kN/m <sup>2</sup>
$\phi_u$	0
$\phi$	26°

Table 2. Modeling conditions of soft soil used

Model 1(D1)	Drained parameters without allowing time for consolidation
Model 2 (D2)	Embankment construction rate 0.5m/week, coupled consolidation
Model 3(U1)	Undrained Parameters

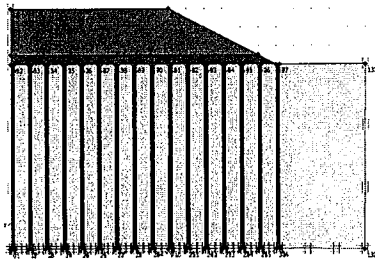


Fig.1 - Model Preparation for the analysis

## 5. COMPARISON OF RESULTS

### 5.1. Different Analysis Models Used

Results are obtained with limit equilibrium approaches; Average shear stress method (M1), Embankment loading without considering stress concentration effect (M2) and Embankment loading with considering stress concentration effect (M3). In M2 and M3 stone columns were idealized by strips in a plane strain formulation (Figure 2). Stress concentration effect is also illustrated in the figure.

Average strength calculation and Stress concentration factor calculation can be shown as follows.  
Average parameters calculation;

$$\phi_{avg} = \tan^{-1}(\mu_o a_o \tan \phi_o) \dots \dots \dots \text{Eq.1}$$

$$\gamma_{avg} = \frac{A_s \times \gamma_{stone\ column} + A_c \times \gamma_{soil}}{A_s + A_c} \dots \dots \dots \text{Eq.2}$$

$$c_{avg} = (1 - a_s) c \dots \dots \dots \text{Eq.3}$$

Stress concentration factor;

$$n = a + b \left( \frac{E_s}{E_c} \right) \dots \dots \dots \text{Eq. 4}$$

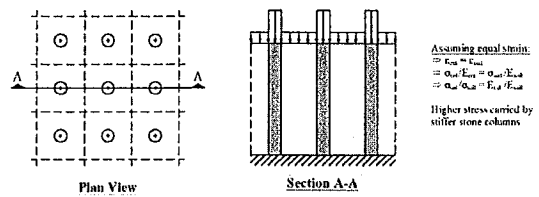


Fig.2 – Stress distribution of stone columns

Results are obtained with the Finite Element approach through PLAXIS with modeling conditions D1, D2 and U1 as in Table 2.

The analyses were done varying the friction angle of stone Column material was considered 32°- 40° simulating stone column materials compacted to different densities.

Finite element analysis with PLAXIS does not provide a direct value of FOS. It was obtained through the  $c, \phi$  reduction technique available in the program. The shear strength parameters are reduced gradually by a factor and the value of the factor when the displacement increased rapidly is taken as the factor of safety.

### 5.2. Comparison of PLAXIS Results

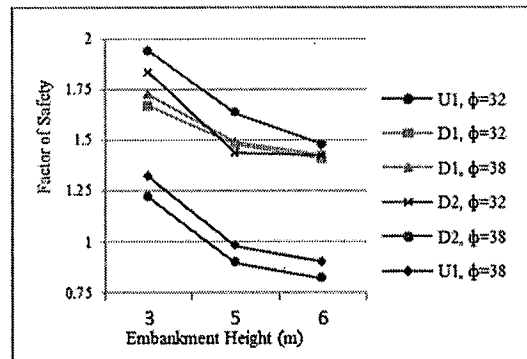


Fig.3 – FOS Variations of Plaxis Models

In all analyses, the FOS reduced as the height of the embankment height increased. Stone columns with greater strength (higher  $\Phi$  value) gave a greater FOS in general. But at higher embankment heights values got quite close. The lower FOS given by D2 compared to D1 can be explained by the fact that pore pressure dissipation was not modeled in D1. In D2 there was some time for pore pressure dissipation with the specified rate of construction. As the construction progressed there are significant accumulated pore pressures and values by D1 and D2 became closer.



Ideally, the results of D1 and U1 should be same as pore pressure dissipation was not permitted in both. But the results obtained by U1 are much lower than those by D2. This variation is most likely due to the incompatibility in the set of undrained parameters and drained parameters used for the analysis.

A sensitivity analysis was done on this regards showed that the undrained cohesion value should be increased to around 15 kN/m<sup>2</sup> to be compatible with drained parameters.

### 5.3. Comparison of the Simplified Methods

The FOS values obtained from different limit equilibrium approaches were compared in Fig. 4

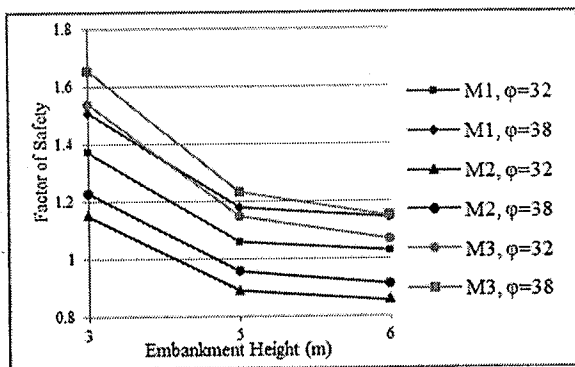


Fig.4-Comparison of Simplified Methods

In all models FOS increased with the increased density of the stone column (from  $\Phi=32$  to 38). It can be seen that the M3 gives higher FOS than the other two methods, but are closer to M1. But the values given by two methods, M3 and M1 are much closer when the embankment height is increased. But when compared with the other two methods, M2 gives much lower FOS values and hence conservative designs. M1 is much easier to implement and it shows that when the stress concentration is considered in computation of average strength parameters, results closer to more tedious strip method with stress concentration effect can be obtained.

### 5.4. Comparison of the Results of the LE analyses with FE analyses

Stone column material  $\phi=32$  was used for the comparison. Actual condition is more closely modeled by D2. The limit equilibrium methods M1, M2 and M3 do not account for any pore pressure dissipation during the construction. The FOS values given by drained FE model is much greater as seen in fig.5. If the limited consolidation

that has taken place and the resulting gain in undrained shear strength within that period had been accounted the results of M1, M2 M 3 could be much closer to D2. This is illustrated in fig. 6.

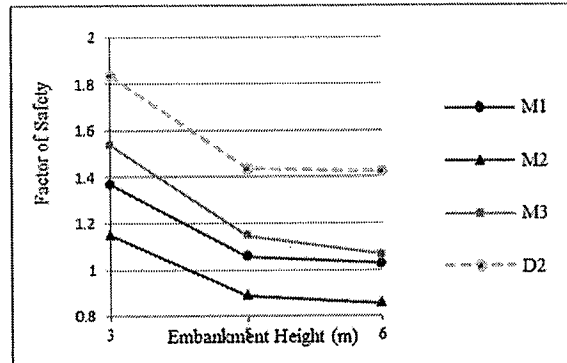


Fig.5-Comparison of Different Methods with PLAXIS Drained Model

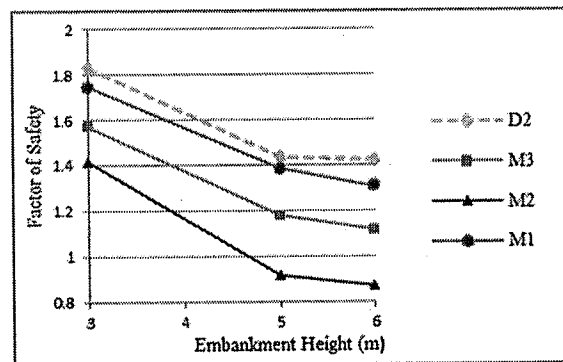


Fig.6-Comparison of Different Methods with Improved Undrained Shear Strength Values

### 5.5. Comparison of Stress Concentration Effect

In limit equilibrium approach normally a constant stress concentration factor has to be assumed. Based on empirical factors a value of 2.1 was used in the analyses done with Slope/W. The stress distribution is calculated in the PLAXIS without making any assumptions. The vertical stresses on stone columns are much higher than on soft clay as seen in Fig. 7 for embankment height of 3m. The ratio-the stress concentration factor is not constant throughout the section. Therefore, an average value is calculated. The values calculated for 3m, 5m and 6m embankment heights are 5.4, 8.5 and 11.5 respectively. Vertical stress distribution for 5m embankment is shown in fig.8. This indicates that the stress concentration factor increased when the embankment height increases. Stress concentration factor calculated using the empirical equations is much smaller than the values given by the finite element computation.

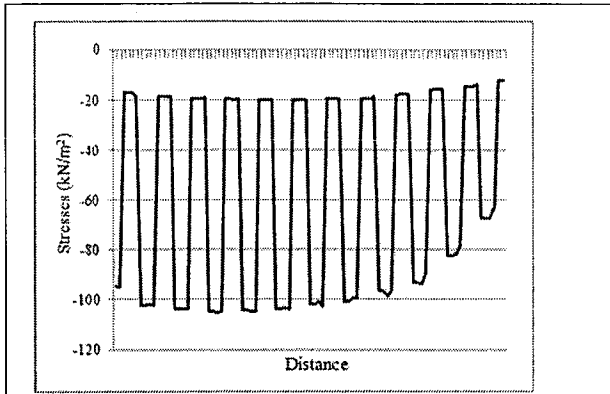


Fig.7-Stress Distribution Under the Embankment for 3m Embankment Height

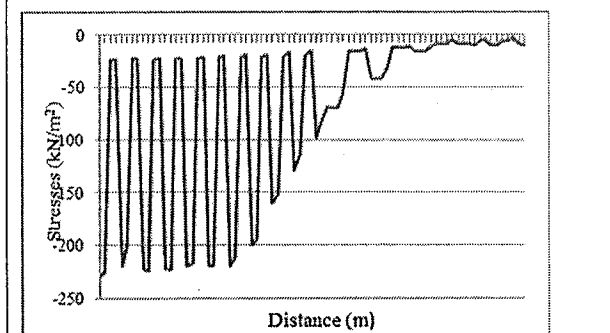


Fig.8-Stress distribution under the embankment for 5m embankment height

5.6. Analysis incorporating the change of Stress Concentration factor in Limit Equilibrium Approach

Another analysis was carried out with limit equilibrium approach accommodating the change of stress concentration factor with the embankment height. In this analysis stress concentration factors of 5.4, 8.5 and 11.5 were used for embankment heights 3m, 5m and 6m respectively. In figure 9 the results are compared with those of D2 which is the most realistic method.

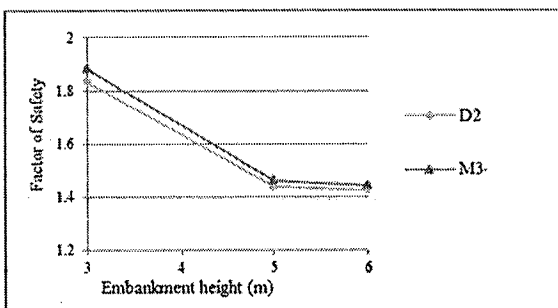


Fig.9-Comparison of PLAXIS drained Model with LEA

It can be observed that the results of limit equilibrium analyses match well with PLAXIS Drained model if all the effects such as strength gain and stress concentration factor variation are accounted.

6. CONCLUSION

From the results obtained, it can be said that the method which consider the stress concentration effect gives more reliable results in the analysis but only when the incompatibilities with data are removed and close stress concentration factors are used. There is no practice of changing the stress concentration factor with the embankment height in the limit equilibrium approach. An empirical equation provides a stress concentration factor based on soil stiffness ratio. PLAXIS analysis indicates that an updating of stress concentration factor is needed when the embankment height increases.

Therefore, further studies need to be done on calculate stress concentration factor. These values can be obtained from the experimental studies and compared with the finite element simulations done with PLAXIS. Such studies will help to optimise the analysis techniques.

ACKNOWLEDGEMENT

The author is grateful to Professor S.A.S. Kulathilaka, University of Moratuwa for his valuable guidance and support for this Research.

REFERENCES

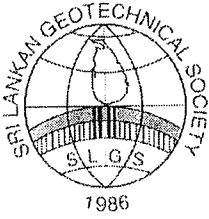
Ellouze, S., Bouassida, M., Hazzar, L., & Mroueh, H. (2010). On settlement of stone column foundation by Priebe's method. Proceedings of the ICE-Ground Improvement, 163(2), 101-107.

Karun Manil, Nigee.K (2013). A study on ground improvement using stone column technique. Proceedings of the IJIRS- Engineering Technology. Volume 2, Issue 11, 6451-6456

McKelvey, D., Sivakumar, V., Bell, A., & Graham, J. (2004). Modelling vibrated stone columns in soft clay. Proceedings of the ICE-Geotechnical Engineering, 157(3), 137-149.

Mokhtari, M., & Kalantari, B. (2012). Soft soil stabilization using stone columns—A review. Electronic Journal of Geotechnical Engineering, 17, 1459-1456.

Wickremasinghe R.V (2013). Study of stone column design methods, Undergraduate Research, University of Moratuwa



# Optimization of Landfill Final Cover Based on Gas Exchangeable Properties of Soil

M.H. Samarakoon and E.B.S. Madushan

*Department of Civil and Environmental Engineering, Faculty of Engineering, University of Ruhuna, Sri Lanka.*

**ABSTRACT:** Solid waste inside the landfill undergoes complex sequence of reactions. These reactions can be mainly categorized into two groups namely aerobic and anaerobic. In both these reactions, carbon dioxide generates as one of the resultant gases. However in anaerobic condition, methane gas which is more critical for greenhouse effect produces and emits to the atmosphere through final soil cover. Gas exchange through final cover soil is mainly governed by two gas transport mechanisms namely advection and diffusion. Hence it is very important to study the gas exchangeable properties of final cover soil of an engineered landfill. In this research study, the effect of compaction energy, grain size distribution and moisture content of final cover soil on gas transport parameters were studied. Based on the results it can be concluded that, in order to enhance the aerobic condition inside the landfill cover, it is important to compact the final cover soil in the dry side of optimum moisture content with intermediate particle range. Further, obtained results were compared with the existing gas transport models and results illustrated that findings of this research study were well agreed with the existing models.

## 1. INTRODUCTION

Municipal solid waste inside the landfill undergoes complex sequence of biological and chemical reactions under anaerobic conditions which cause to generate hazardous gasses. Inadequate waste management and disposal practices combined with the climatic changes result in increasing environmental problems (Visvanathan et al., 2004). Hence it is necessary to pay special attention on controlling the emission of landfill gases, since it causes global warming.

Methane is 25 times critical than CO<sub>2</sub> for greenhouse effect (Wickramarachchi et al., 2011). The major factors governing the CH<sub>4</sub> oxidation process in landfill final cover soils are soil texture, porosity, air content, bulk density, organic content, moisture content, soil temperature, pH, nutrients, and O<sub>2</sub> and CH<sub>4</sub> concentrations (Abushammala et al., 2014). Since most of the gasses emit through the final cover of a landfill, it is very important to study the gas exchangeable properties of landfill final cover soil.

The design of cover systems to accommodate landfill gas control requires an understanding of the physical, chemical and biological processes governing gas migration. (Hettiaratchi et al., 1998). Advection and the diffusion are the two mechanisms of gas transportation through the final cover soil. Diffusion is a process of movement of particles from high concentration to low concentration. Therefore, molecules of methane and carbon dioxide diffuse from the landfill gas to the air. Simultaneously, atmospheric air, mainly oxygen diffuses to waste body and it helps to increase the

aerobic decomposition of organic matter (Kumari and Sanjaya, 2013). The soil-gas diffusion coefficient ( $D_p$ ) and its dependency on soil physical characteristics governs the diffusive transport of oxygen, greenhouse gasses through landfill final cover. Fick's law is used to calculate the gas diffusion coefficient ( $D_p$ ). Soil-gas diffusivity ( $D_p/D_o$ ) is defined as the normalized ratio between soil-gas diffusion coefficient ( $D_p$ ) and gas diffusion coefficient in free air ( $D_o$ ). There exist developed models for soil gas diffusivity as a function of soil type and air content ( $\epsilon$ ). Buckingham (Kumari and Sanjaya, 2013) suggested that soil gas diffusivity follows power law function of soil air content such that in Eq. (1),

$$\frac{D_p}{D_o} = \epsilon^x \quad (1)$$

Where  $\epsilon$  is the soil air content and  $x$  is an exponent characterizing pore connectivity.  $x=2$  for Buckingham model and  $x=1.5$  for Marshall model. Penman further modified the model by removing exponent but inserting 0.66 as coefficient for air content (Kumari and Sanjaya, 2013).

Advection is the gas transportation mechanism of flowing air from high pressure to low pressure. Generally advection of soil is measured in terms of coefficient of air permeability ( $K_a$ ). The theory for the flow of air through soil is based on Darcy's law. Existing general models of air permeability are also based on power law function of soil air content ( $\epsilon$ ), same as air diffusion. The generalized form of such models can be written as,

$$K_a = \alpha \varepsilon^x \quad (2)$$

In Eq. (2),  $\alpha$  is pore connectivity constant and  $x$  is power law exponent which can be either 2 for Buckingham type or 1.5 for Marshall type (Kumari and Sanjaya, 2013).

In this research study, the effect of three soil parameters, such as compaction energy, moisture content and grain size distribution on above mentioned two gas transport parameters were evaluated for commonly available lateritic soil. Finally obtained results were compared with existing models.

## 2. MATERIALS AND METHODOLOGY

### 2.1 Physical properties

Commonly available lateritic soil was used as the candidate material. Physical properties of laterite soil are illustrated in Table 1. Soil classification according to Unified Soil Classification System (USCS) is also presented in the Table 1 and it was found that soil is poorly graded sand (SP).

Property	Value
Specific Gravity	2.69
Liquid Limit (LL %)	65
Plastic Limit (PL %)	45
Plasticity Index (PI %)	20
Linear shrinkage (%)	5
Coefficient of Uniformity ( $C_u$ )	5.33
Coefficient of Curvature ( $C_c$ )	1.33
Gravel Content (%)	0
Sand Content (%)	98.34
Fine content (%)	1.66
Classification according to USCS	SP

Table 1. Physical properties of lateritic soil

### 2.2 Grain size distribution

Three ranges of particle sizes were used to determine the gas transport parameters under the objective of finding the effect of grain size. The particle size ranges are,

1. Less than 2.36 mm
2. Between 2.36 and 4.75 mm
3. Between 4.75 and 9.5 mm

Above three ranges of particle sizes were selected, because the size of the mould used for sample preparation is small and also the two apparatus used to determine gas transport parameters

mainly designed for the small mould. Particle size distribution curve for selected material together with three ranges is shown in Fig. 1.

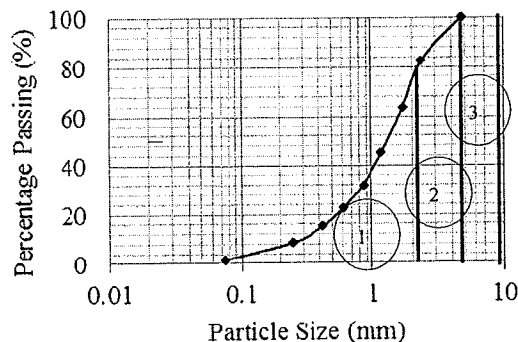


Fig.1 Particle size distribution of lateritic soil

### 2.3 Compaction energy

Three types of compaction energy levels such as standard, intermediate, modified were used to find the effect of compaction on gas transport parameters. Summary of the energy levels used is illustrated in Table 2.

	No of blows per layer	No of layers	Energy (kJ/m <sup>3</sup> )
Standard energy	25	3	583
Intermediate energy	40	5	1554
Modified energy	69	5	2681

Table 2 Compaction energy levels

All soil samples were prepared in 100 cm<sup>3</sup> moulds using a specially designed hammer. The weight of the hammer is 0.524 kg and drop height is 150mm. For a particular test, soil samples were prepared representing both dry and wet side of optimum moisture content.

After the preparation of soil samples, coefficient of air permeability ( $k_a$ ) and diffusion coefficient ( $D_p$ ) were measured using air permeameter and diffusion chamber respectively. Since moisture content was already varied during sample preparation, compaction energy and particle sizes were changed to find the effect on  $k_a$  and  $D_p$ .

### 2.4 Determination of gas transport parameters

coefficient of air permeability ( $k_a$ ) was measured in the laboratory using air permeability setup as illus-

trated in Fig. 2, in which air is flowing at a given inlet pressure through soil samples. Using the pressure gauge, pressure difference between top and bottom of the sample was measured to calculate  $k_a$  value based on Darcy's law (Curie, 1960).

Diffusion coefficient ( $D_p$ ) was measured using the diffusion chamber as illustrated in Fig. 3. Initially the closed chamber was flushed with  $N_2$  and all the  $O_2$  (used as the tracer gas) inside the chamber was removed. Then the soil sample was fixed to the apparatus, keeping the top surface of the sample open to the atmosphere. Once the chamber was opened, atmospheric air is diffused to the chamber through the soil sample. Change of  $O_2$  concentration was measured as a function of time using the  $O_2$  sensor connected to the diffusion chamber through a data logger, and then  $D_p$  was calculated (Wickramarachchi et al, 2011). The gas diffusion coefficient of oxygen in free air ( $D_o$ ) at  $20^\circ C$  was taken as  $0.20 \text{ cm}^2/\text{s}$  (Curie, 1960).

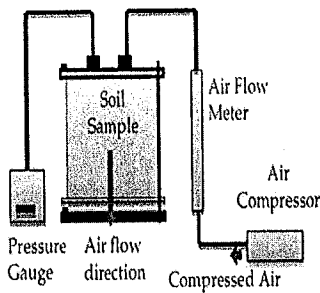


Fig.2 Air permeability setup

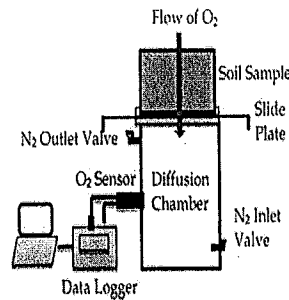


Fig. 3 Gas diffusion setup

### 3. RESULTS AND DISCUSSION

#### 3.1 Soil-air permeability

##### 3.1.1 Effect of compaction energy on air permeability

Fig. 4 illustrates the variation of measured air permeability ( $k_a$ ) of soil samples with particle size less than 2.36mm under different energy levels as a function of moisture content.

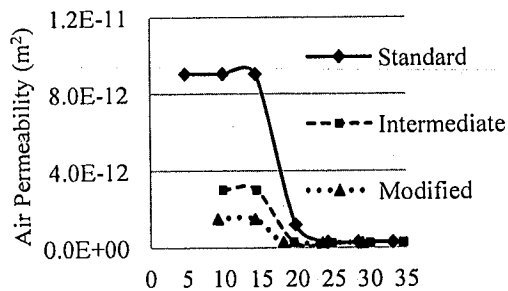


Fig.4 Variation of  $K_a$  of  $K_a$

with moisture content over different energy levels

It can be noted that,  $k_a$  decreases with the increase of energy from standard to modified level. When energy increases compaction level increases and void space inside the soil sample decreases. Hence air moving paths are interrupted by solid particles which tend to decrease the air permeability. Further it can be seen  $k_a$  has been significantly decreased in the wet side of optimum moisture content.

##### 3.1.2 Effect of grain size distribution on air permeability

Fig. 5 illustrates the variation of air permeability ( $k_a$ ) with moisture contents of the soil for three different particle sizes under standard energy level. It can be noted that the smallest sieve range (less than 2.36mm) is shown the lowest variation of air permeability while middle sieve range (2.36 – 4.75 mm) is shown the highest variation of air permeability. Although 4.75 – 9.5 mm range have larger grain size particles, when compaction energy is applied some large particles are broken into small particles. It will cause well graded distribution in the sample mould which fill the porous space by reducing air permeability.

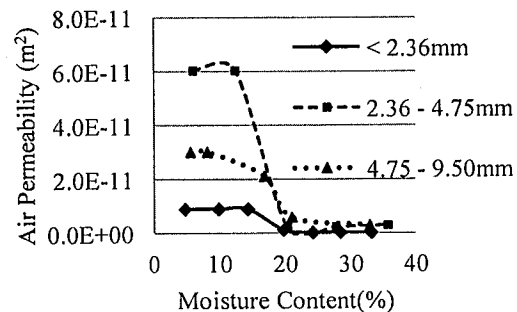


Fig.5 Variation of  $K_a$  with moisture content over different particle sizes

Further, similar to the Fig. 4,  $k_a$  has been significantly reduced when the moisture content is more than the optimum moisture content. This is a clear indication that in order to enhance the advection, it is important to compact the final cover soil in the dry side of optimum moisture content.

#### 3.2 Soil-gas diffusivity

##### 3.2.1 Effect of compaction energy on diffusivity

The variation of soil gas diffusivity ( $D_p/D_o$ ) with moisture content for three types of energy levels are depicted in Fig. 6.

When energy level increases, diffusivity decreases by keeping similar variation with moisture content.

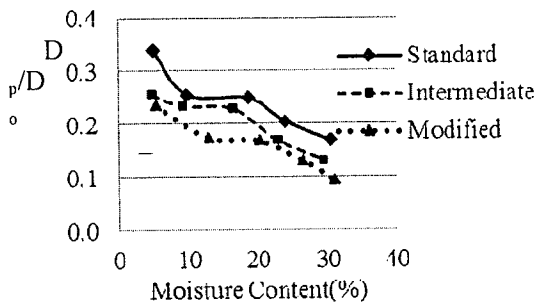


Fig.6 Variation of  $D_p/D_0$  with moisture content over different energy levels

3.2.2 Effect of grain size distribution on diffusivity

Fig. 7 illustrates the variation of diffusivity of soil samples with moisture contents of the soil for three different particle sizes under same energy level. It can be seen that intermediate particle size (2.36 – 4.75 mm) shows the highest variation which is much similar to the air permeability behavior.

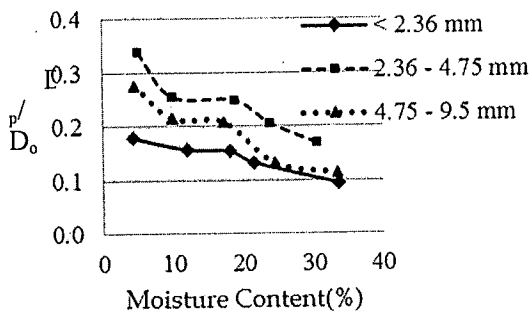


Fig.7 Variation of  $D_p/D_0$  with moisture content over different particle sizes

3.3 Comparison of results with existing models

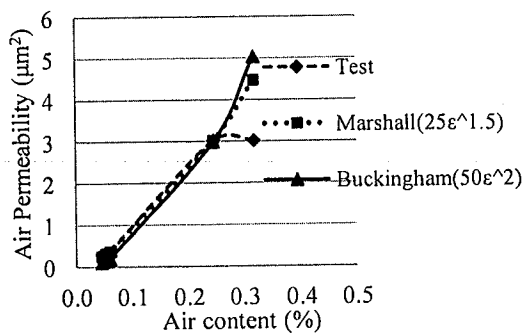


Fig.8 Comparison of air permeability vs. air content results with numerical models (Intermediate energy)

In order to verify the laboratory experimental results, data were compared with the existing models. Fig. 8 illustrates the comparison of air permeability values over air contents with existing models namely Marshall and Buckingham (Wickramarachchi et al., 2011). Those models follow the power law function of soil-air content ( $\epsilon$ ). Marshall model ( $x=1.5$ ) and Buckingham model ( $x=2$ ) was applied here with ent  $\alpha$  values in  $K_a = \alpha \epsilon^x$  in order to verify air permeability of soil samples. The  $\alpha$  constant has been changed to find out the exact matching model with the obtained results while keeping exponent  $x$  constant. According to the graph, it shows that those two models with applied values can be used to verify air permeability parameters of lateritic soil. Similar results with respect to diffusion can be observed.

4. CONCLUSIONS

A series of laboratory tests were conducted in order to study the effect of energy level, particle size and moisture content of final cover soil in an engineered landfill on gas transport parameters. Based on this research study, it was revealed that to enhance the methane oxidation process within the landfill, it is very important to compact the final cover soil in dry side of optimum moisture content which increases air permeability as well as diffusivity. Further in order to enhance the gas transport parameters namely advection and diffusion, final cover soil shall be compacted using standard energy level with intermediate particle sizes for cover material. The findings of this research study were well agreed with existing power law models such as Buckingham and Marshall.

REFERECES

Abushammala, MFM, Basri, NEA, Danilwan and Younes, MK, "Methane Oxidation in Landfill Cover Soils", Asian Journal of Atmospheric Environment, Vol. 8-1, 2014, pp. 1-14.

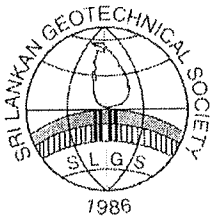
Curie, J.A. (1960), *Gaseous Diffusion in Porous Media, Part 1- A non-steady state method*, British Journal- Applied Physics, vol. 11, pp.314-317.

Hettiaratchi, JPA, Perera, MDN, Viswanthan, C, & Pokhrel, D, "Design of landfill cover systems incorporating soil methanotrophy for methane emission mitigation", In Fourth International Symposium on Environmental Geotechnology and Global Sustainable Development, Boston, MA, Aug. 1998, pp. 1540-1550.

Kumari, WGP and Sanjaya, SKE, "Selection of Suitable Material for Final Cover of an Engineered Landfill in Dry Zone", Undergraduate research project thesis, University of Ruhuna, 2013.

Viswanthan, C, Tbtimthai, O and Kuruparan, P, "Influence of Landfill Top Cover Design on Methane Oxidation", Third Asian- Pacific Landfill Symposium, 2004, pp.387-394.

Wickramarachchi, PNK, Kawamoto, K, Hamamoto, S, Nagamori, S, Moldrup, P, Komatsu, T, "Effects of Dry Bulk Density and Particle Size Fraction on Gas Transport Parameters in Variably Saturated Landfill Cover Soil" Journal of Waste Management, vol31, no 12, 2011, pp. 2464-2472.



# Effect of Rainfall on Slope Failures in Unsaturated Soil

A.B.K.A. Lakmali and H.B.P. Raveendra

*Department of Civil and Environmental Engineering, Faculty of Engineering, University of Ruhuna*

**ABSTRACT:** Slope failures and landslides in unsaturated soil are influenced by geologic, topographic and climatic factors. The main causative factor for these slope failures in the unsaturated soil is the rainfall. Rain-water infiltration causes a loss of matric suction creating positive pore water pressures with the development of the perched water table. This paper discusses about the geotechnical properties, specially the shear strength parameters of unsaturated soil and how they get changed with the rainfall and the soaking effect. With the change of shear strength parameters of soil, the stability of slopes with unsaturated soil is varied. In this research study, the mechanism of slope failures in unsaturated soil, was studied considering the variation of shear strength parameters on moisture content of soil. The effective cohesion seems to be decreased by 85% and the friction angle by 28% after 6 days of continuous rainfall. Slope stability analysis was done using SLOPE/W software incorporating the seepage analysis using SEEP/W software.

## 1. INTRODUCTION

Rainfall-induced slope failures are one of the most common natural hazards in tropical countries. As a tropical country in South Asia, Sri Lanka has been faced many rain-induced slope failures which had created much adverse effects. During the last decade, landslide is one of the most catastrophic natural hazards in Sri Lanka (Disaster Management Centre, 2009).

According to the statistics, Sri Lanka has been experiencing landslides in the areas of central hill country and south western region since early eighties. Mainly natural landslides are associated with the periods of heavy rainfall. History clearly shows that continuous and intensive rainfall has triggered a number of catastrophic landslides events in the hill region of Sri Lanka (Disaster Management Centre, 2009). North-East and South-West monsoon which bring heavy rainfall to the country badly affect too many areas in the country causing many landslides.

The most severe landslide in the history of Sri Lanka was occurred at Meeriyabedda in Koslanda on 29th October 2014 around 7.30 a.m., which affected around 330 people of 57 families in Ampitikandatea estate. The landslide occurred near the town of Haldummulla and mud and debris buried approximately 150 houses and potentially more than a hundred residents. Some houses in the area have been buried in mud as deep as 9 metres (Geological Survey and mines bureau of Sri Lanka, 2014).

In unsaturated soil, there are higher inter-particle forces due to the negative pore-water pres-

sure. The behavior of water in unsaturated soil is related to phenomena such as vapor pressure, evaporation, suction and cavitation (Sahin, 2013). The main cause for these failures is the loss of matric suction due to the development of perched water table and as a result of infiltration of rain water (Li et al., 2005).

As such, research on rainfall induced slope failures will be more effective in future disaster management in the country. The objectives of this research is to study the variation of shear strength parameters with the moisture content and stability of slope due to development of perched water table affected by the rainfall, taking Meeriyabedda landslide as a case study. Ultimate intention was to determine the shear strength parameters during the failure of Meeriyabedda landslide and the percentage reduction in those shear strength parameters.

## 2. MATERIALS AND METHODOLOGY

Meeriyabedda landslide site was visited and collected soil samples as much as possible representing the area. Basic properties of Meeriyabedda soil were determined by using various laboratory tests and are shown in Table 1. Grain size distribution of Meeriyabedda soil which was obtained from sieve analysis is illustrated in Fig. 1.

From Fig. 1, it is clear that the soil is composed of a heterogeneous range of large particles and sediments ranging from silt to rock fragments of various sizes. So it is obvious that the soil is a colluviums.

Table 1 Basic properties of Meeriyabedda soil

Property	Result
Liquid Limit	63%
Plastic Limit	40%
Plasticity Index	23%
Linear shrinkage	6.62%
Specific Gravity	2.7
Bulk density	1600 kg/m <sup>3</sup>
Coefficient of saturated permeability	7.81×10 <sup>-6</sup> cm/s

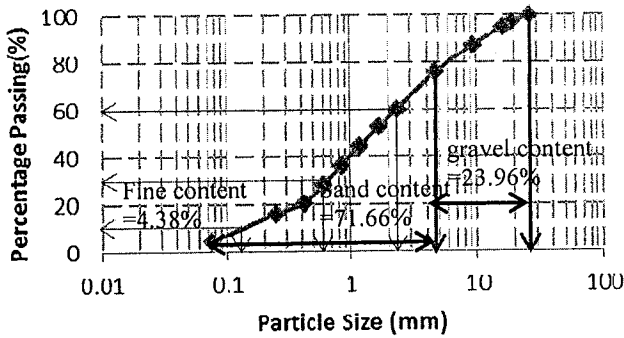


Fig. 1 Grain Size Distribution

2.1 Determination of Shear Strength Parameters

Variation of shear strength parameters with the moisture content and soaking effect was determined for the colluvium soil at Meeriyabedda. As the first approach, series of direct shear tests were conducted by varying the moisture content of the soil maintaining the field density. Tests were conducted for 20, 40, 60 and 80 kPa of normal stresses for particular moisture content with a 0.15 mm/s shearing speed and the shear strength parameters corresponding to that moisture content were determined. Cohesion and the friction angle for several moisture contents were determined using the direct shear test.

As the second approach, soaking effect on the shear strength parameters of the Meeriyabedda soil was determined. Soil samples of 89mm diameter and 50 mm thickness were compacted to the field density in a sampling ring. They were soaked in a water bath for 1, 2, 3, 4, 5 and 6 days and direct shear tests were conducted for each soaking day

following the same procedure as in the first approach. The sample preparation to check the soaking effect is shown in Fig. 2. The moisture content of the soil samples corresponding to the each soaking day was determined. The shear strength parameters corresponding to each soaking day were determined from the series of direct shear tests.

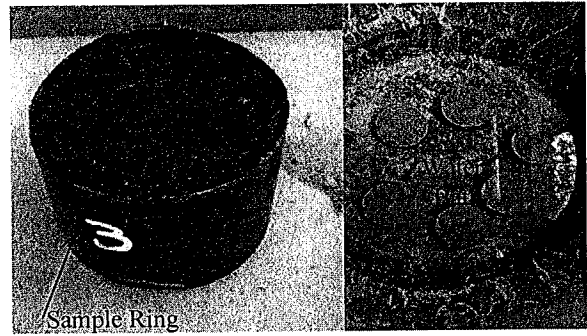


Fig. 2 Sample Preparation for Direct Shear Test

2.2 Slope Stability Analysis

The slope stability analysis was conducted using the SLOPE/W software incorporating the seepage analysis results of SEEP/W software. Three rain events of 100mm/day, 167mm/day and 300mm/day and initial water tables of 10m, 30m and 60m below the ground surface were selected to study the development of the perched water table on the slope of Meeriyabedda under the different rainfalls intensities and initial water tables. Fig. 3 shows the slope geometry and the boundary conditions of Meeriyabedda slope that were used in the analysis.

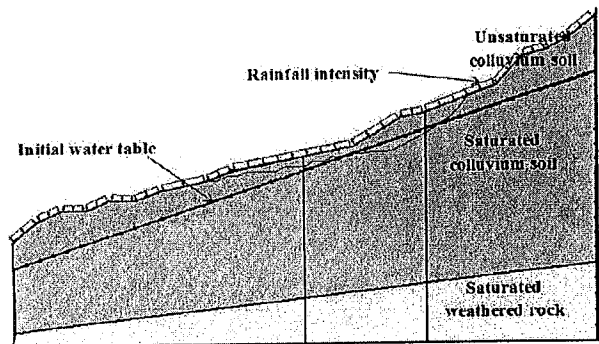


Fig. 3 Slope Geometry and Boundary Conditions

In SEEP/W software the slope geometry and the boundary conditions were allocated initially. The initial water table was assigned and analysis was done by varying the rainfall intensities. From the seepage analysis, the pore water pressure variation and the development of the perched water table was determined. Further, by varying the initial water table, seepage analysis was conducted.



Using the parent analysis of SEEP/W, results were incorporated in SLOPE/W. Then the stability of the slope under these different conditions was checked and the variation of Factor of Safety was determined. In slope stability analysis, material properties and the corresponding shear strength parameters which were determined earlier was assigned in the SLOPE/W software.

The actual failure surface which was needed for analysis was obtained from the topographic analysis from photos of the Aerial Survey from the Helicopter (JICA, 2014) and the analysis was done until the critical failure surface obtained from the slope stability analysis equals to the actual failure surface varying the number of soaking days and the shear strength parameters. The shear strength parameters which were used in the analysis when the critical failure surface equals to the actual failure surface was taken as the shear strength parameters during the failure.

### 3. RESULTS AND DISCUSSION

#### 3.1 Variation of Shear Strength Parameters with Moisture Content

The variation of friction angle and cohesion with respect to moisture content are shown in Fig. 4 and Fig. 5 respectively. Further, effect of soaking on shear strength parameters is also presented. It can be noted that with the increase of degree of saturation due to soaking, shear strength parameters were significantly decreased.

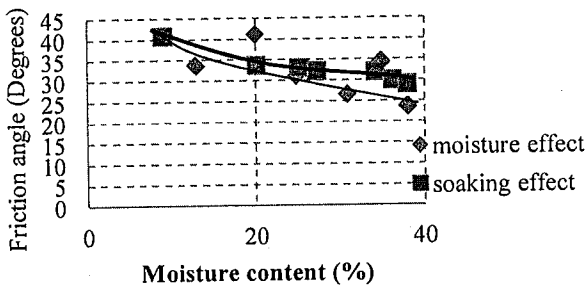


Fig. 4 Variation of Friction Angle with Moisture Content

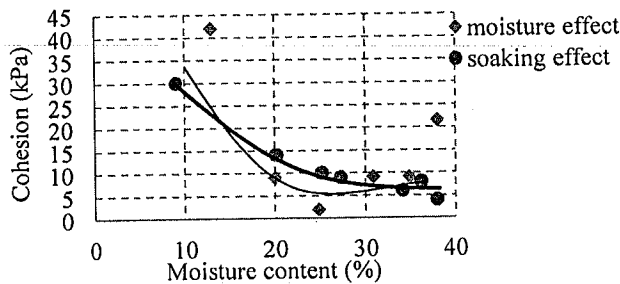


Fig. 5 Variation of Cohesion with Moisture Content

It can be observed that, due to increase of moisture content (due to soaking) friction angle has been significantly reduced when the moisture content reaches to about 40% after 6 days of soaking. Similar behavior can be noticed in the cohesion as well, where cohesion gradually decreases with the increase of moisture content. When it reaches to 40% moisture content 28% reduction has occurred in the friction angle and 85% reduction has occurred in the cohesion.

#### 3.2 Development of Perched Water Table

Seepage analysis using SEEP/W software produces the perched water table. Fig. 6 shows the perched water table that was developed when an average rainfall of  $1.93 \times 10^{-6}$  m/s was continued for 6 consecutive days.

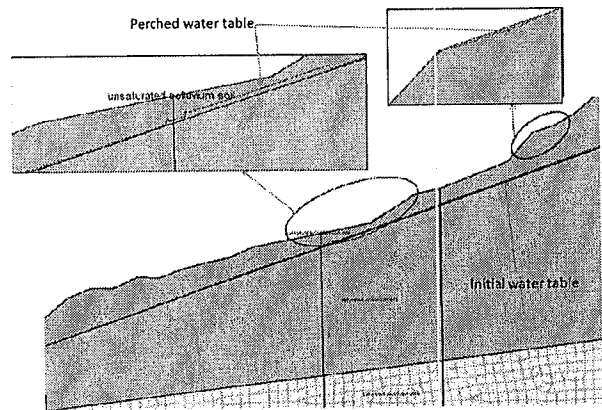


Fig. 6 Development of Perched water table

From the Fig. 6, it is clear that the initial water table has risen up after the continuation of the rainfall for 6 consecutive days. Initially the water table was at 30 m below the ground level. The water table has risen up from the existed water level and in some places it is noticed that perched water table has developed near the ground surface also. Development of perched water table for several other rain events was also occurred in the same manner.

Fig. 7 depicts the variation of pore-water pressure with the progression of the rainfall along a section of the slope. It shows that the negative pore water pressure in the unsaturated region above the water table reaches zero pore water pressure near the ground surface. The reason for the phenomena may be due to the rain fall or the perched water table that was developed with the rain fall. The pore water pressure below the water table is positive.

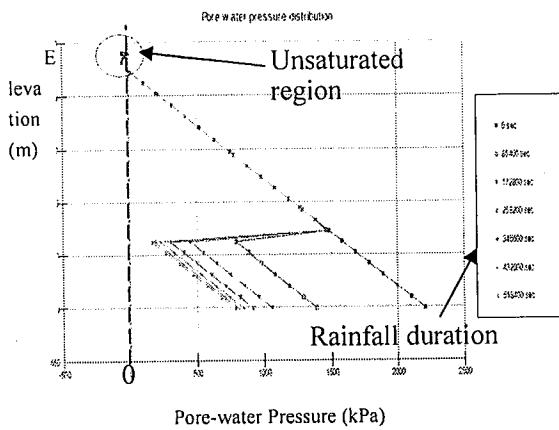


Fig. 7 Pore-water Pressure distribution

### 3.3 Variation of Factor of Safety with the Soaking Time and Rainfall Intensity

The variation of Factor of Safety (FOS) with the number of soaking days for different rainfall intensities is depicted in Fig.8. It is clear that initially the slope is stable under dry condition; however with the increase of the number of soaking days the slope becomes unstable (FOS has been dropped below 1.0). Effect of rainfall intensity on FOS is also presented in the figure, where higher rainfall intensity shows significant reduction in FOS with soaking time. This may due to the reduction of shear strength parameters under soaking condition as shown in Fig. 4 and Fig. 5.

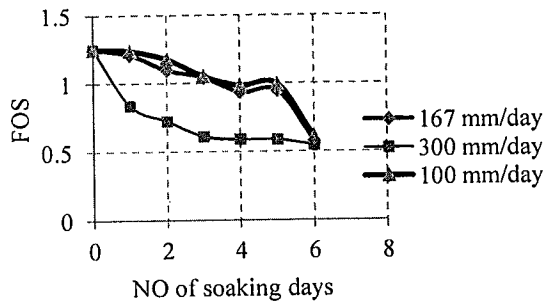


Fig. 8 Graph of FOS Vs. No. of soaking days

## 4 CONCLUSIONS

Effect of moisture content and soaking time on shear strength parameters were studied in this research study. Based on the results, it can be concluded that the steep slopes made of unsaturated soil are stable during the dry season. The main reason behind the stability of steep slopes during the dry period is the matric suction or the negative

pore water pressure. With the rainfall these steep slope become unstable due to the loss of matric suction and development of positive pore water pressure. From the seepage analysis it was very clear that the initial water table had risen up and a perched water table had developed.

Also it is obvious that the shear strength of unsaturated soil get depleted with the progression of the rainfall. When considering the effect of the variation of shear strength parameters on the stability of the slopes cohesion is much more important than that of friction angle. It is very clear that the Factor of Safety of a particular slope is reduced due to the reduction of the shear strength of unsaturated soil.

During the failure the cohesion was 10kPa and the effective friction angle was  $33^{\circ}$ . Therefore, it can be concluded that during the slope failures, 50-80 % reduction can be observed in the cohesion whereas 20-50 % reduction can be observed in friction angle.

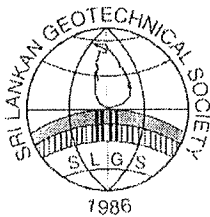
As future directions moisture sensors can be installed in the field and the variation of the shear strength parameters can be monitored. It can be used to develop an early warning system for the slope failures.

## ACKNOWLEDGMENTS

The authors acknowledge all who have supported to make this research a success, in the Department of Civil and Environmental Engineering, University of Ruhuna. The authors specially acknowledge the support received from the National Building and Research Organization (NBRO), for the rainfall data of Poonagala gauging station which were used in the analysis and Japan International Cooperation Agency (JICA) for the topographical map used in the analyses presented in this article.

## REFERENCES

- Disaster Management Centre, 2009, Sri Lanka National Report on Disaster Risk, Poverty and Human Development Relationship
- JICA Technical Cooperation for Landslide Mitigation Project, 2014, Helicopter Survey Report on BadullaKoslanda Landslide
- Li, A. G., Yue, Z. Q., Tham, L. G., Lee, C. F., & Law, K. T., 2005, 'Field-monitored variations of soil moisture and matric suction in a saprolite slope', Canadian Geotechnical Journal 42(1), 13-26.
- Şahin, Y., 2013, 'Laboratory tests to study stability mechanism of rainfall infiltrated unsaturated fine-grained soil slopes developing into shallow landslides and their hydraulic properties', Doctoral dissertation, İzmir Institute of Technology.
- Geological Society of Sri Lanka, 2014, GSSL Newsletter.



# Analysis of Soil-nail Pullout Interaction in Lateritic Soil Using Laboratory Models

B. L. A. Isaka and B. C. Madushanka

Department of Civil and Environmental Engineering, Faculty of Engineering, University of Ruhuna

**ABSTRACT:** Soil-nailing is an effective slope stabilizing technique and soil-nail interaction plays a vital role in designing soil-nailing structures. This study was carried out to determine the pullout resistance of a soil-nail and the load-displacement behaviour of a nail under pulling. Several pullout tests were conducted under different overburden pressures and different saturation conditions on steel bars embedded in compacted soil by preparing a laboratory model. Also the effect of grout interface on pullout resistance was evaluated by introducing a grout interface between nail and soil. Based on the laboratory experiments it was revealed that the experimental peak pullout forces were higher compared to that of the theoretical values and a multiplication factor within a range of 2.0-2.7 was resulted for the experimental to theoretical values. This difference was significant with a grout interface and the multiplication factor increases up to a range of 4.8- 6.0. A two-dimensional *PLAXIS* model was used to validate and analyze the experimental data numerically.

## 1 INTRODUCTION

It is a challenge in geotechnical engineering to stabilize steeper, larger slopes and soil-nailing is an effective slope stabilizing technology which can be used in congested areas with a low cost, less working area and with fast construction (Powell and Watkins, 1992). A common problem that experienced in geotechnical engineering is that the pullout force resulted from field pullout tests are much higher than that of theoretical values used for designs. Therefore, this study was conducted to compare experimental results with the theoretical values and build up a relationship to accurately determine the pullout force in soil nailing in order to perform cost effective designs.

The behavior of a soil-nailed wall is much advanced and several researches have been studied the behavior of a nailed-soil mass (Milligan and Tei, 1998; Junaideen et al, 2004; Pradhan et al., 2006; Hong, 2011; Meetananda et al., 2001). Generally, theoretical pullout force values are calculated based on the equation,

$$F_{theoretical} = \pi dl(c' + \sigma_v' \tan \phi') \quad (1)$$

Where  $c'$ ,  $\phi'$  are effective shear strength parameters (cohesion and friction angle) of surrounding soil,  $\sigma_v'$  is the effective vertical stress,  $d$  is the nail diameter and  $l$  is the nail length. A bond coefficient ( $f_s$ ), was introduced in this research study to the theoretical pullout force values to be equal to the experimental pullout force values. Then field pullout force ( $F_{field}$ ) can be determined as,

$$f_{field} = f_s \times \pi dl(c' + \sigma_v' \tan \phi') \quad (2)$$

Determination of this bond coefficient  $f_s$  was done from this research study as a solution to accurately determine the theoretical pullout resistance. Hence, objectives of the research study can be summarized as;

1. Determination of effect of overburden pressure, degree of saturation and grout interface (interface shear strength parameters) between nail and soil on pullout resistance using a laboratory model setup.
2. Determination of pullout resistance by numerically using *PLAXIS* software.
3. Determination of theoretical pullout resistance accurately by introducing a bond coefficient.

## 2. MATERIALS AND METHODOLOGY

Lateritic soil, commonly available in Sri Lanka was selected as the candidate material. The geotechnical properties of soil were determined in the laboratory and depicted in Table 1. Soil type was classified as poorly graded sand (SP) with little or no fines according to USCS (Unified Soil Classification System).

Table 1 Physical Properties of Lateritic Soil

Property	Value
Liquid Limit (%)	33
Plasticity Index (%)	5
Optimum Moisture Content (%)	22.0
Maximum Dry Unit weight ( $kN/m^2$ )	16.2
Specific Gravity	2.70
Coefficient of Uniformity ( $C_u$ )	4.13
Coefficient of Curvature ( $C_c$ )	1.38
Effective Friction Angle ( $\phi$ )	28°
Effective Cohesion ( $kPa$ )	23

2.1 Mould Preparation

A steel box with internal dimensions of 610 mm × 480 mm × 600 mm was used as the model setup. Lateritic soil was compacted at the optimum moisture content in 50 mm layers. After soil were compacted up to 150 mm height, first reinforcement bar was placed and then filling and compaction were proceeded for next 150 mm thickness. Simultaneously nails were placed at 150 mm spacing with soil filling. A 50 mm distance was kept between the nail and the back boundary of the box. It is believed that such spacing is sufficient to avoid interference due to the nails and the walls of the tank (Junaideen et al., 2004). A pullout jack was fixed to the free end of the nail to pull the nail outwards. The schematic diagram of laboratory experimental setup is shown on the Figure 1.(a) and the photograph of the setup used in the study is shown in

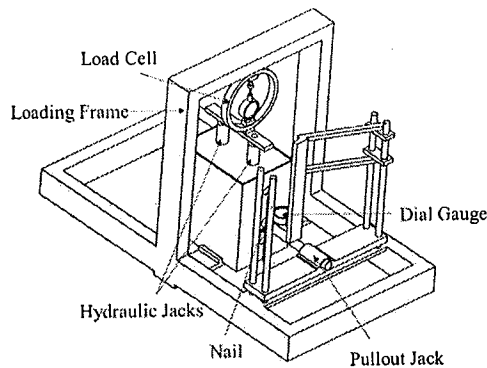


Fig.1.(a)Schematic Diagram of the Model Setup

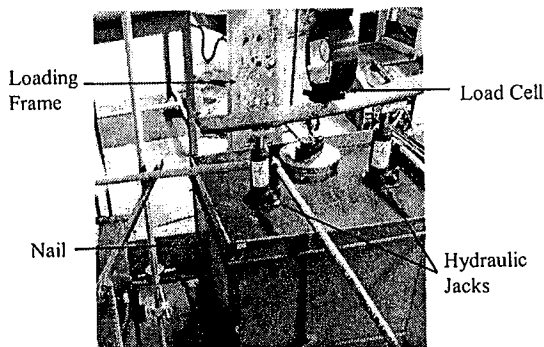


Fig.1.(b)Laboratory Model Setup  
Figure 1.(b).

2.2 Instrumentation and Testing Procedure

Overburden pressure was applied to the box by jacking two hydraulic jacks fixed to a portal frame and monitored by a load cell. A dial gauge was fixed to the nail to monitor the horizontal displacement of the nail during pulling. Pulling out of the nail was done by a pullout jack and the hydraulic pressure required in nail pulling was recorded from a pressure gauge connected to the jack. Before proceed the test, a calibration test was done to

the pullout jack to determine the force corresponds to the recorded fluid pressure. The pullout test was conducted in a displacement controlled manner by jacking the pullout jack.

The top most nail was tested first. The horizontal displacement of a particular nail was monitored up to a maximum displacement of 25 mm or until loss of soil-nail interaction. Series of pullout tests were conducted under different overburden pressures as well as different saturation conditions. Different saturation conditions were maintained by ponding water over the tank for few days.

In order to study the effect of soil-grout interface on pullout resistance, pullout tests were conducted by introducing a grout interface between soil and nail. A 25 mm diameter holes were created in the soil mass during compaction and nails were placed at the center of the hole using centralizers. Cement with water: cement ratio of 0.45 was inserted into the holes manually. Since cement/concrete achieves 75% of compressive strength after 2 week time, pullout tests of these specimens were conducted after two weeks of grout placement.

2.3 Numerical Analysis

Numerical modeling was done simulating the laboratory conditions using PLAXIS software in order to verify the laboratory experimental results. The input geometry of the model is shown in the Figure 2. A prescribed overburden pressure was assigned to the input geometry. Model was analyzed from Mohr-Coulomb failure criteria. The mobilized interface forces were taken from the model at each given displacement. By introducing a separate soil-nail interface, frictional surface between nail and soil was modeled.

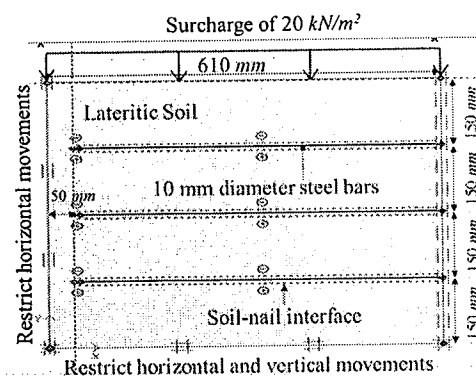


Fig. 2 Input Geometry to PLAXIS Model

Pullout forces and interface forces were obtained by applying subscribed displacements to the free end of the nail in the geometry. Horizontal displacements were varied up to 5 mm with 1 mm interval and the frictional stress developed at the soil-nail interface was resulted from the model analysis. The model was run varying the overbur-

den pressure from  $20 \text{ kN/m}^2$  to  $80 \text{ kN/m}^2$  and for each overburden pressure, behavior of 3 nails were analyzed. First, the prescribed displacement was given to the top most nail, then for the middle nail and finally for the bottom most nail. The analysis was done in *Staged Construction Mode* and the stresses at each phase were resulted from the analysis.

### 3. RESULTS AND DISCUSSION

#### 3.1 Variation of Pullout Force with Nail Displacement

The typical variation of pullout force with nail displacement is shown in the Figure 3. Irrespective of the nail location, all nails showed the same behavior. It can be seen that pullout force increased up to a peak value, and then reduced with nail displacement. This peak pullout force can be considered as the maximum pullout resistance that mobilized on the interface. Nail 1, 2, 3 represents top, middle and bottom nail respectively.

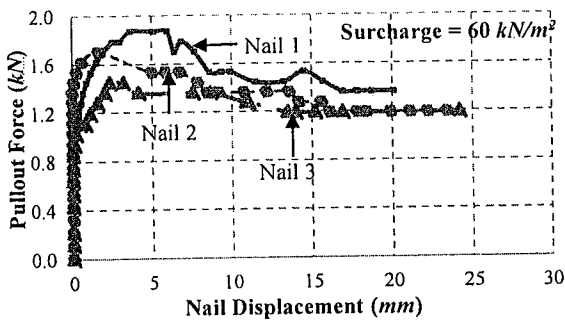


Fig.3: Pullout Force Variation over Nail Displacement

Both experimental and theoretical peak pullout force values calculated based on Equation 1 were increased with the increase of overburden pressure as illustrated in Figure 4. It is very clear that theoretical pullout resistance is much lower than that of experimental results. In order to identify the difference, a multiplication factor was introduced to theoretical pullout force so that equals to the experimental results and it was found that it lies within a range of 2.0 - 2.7.

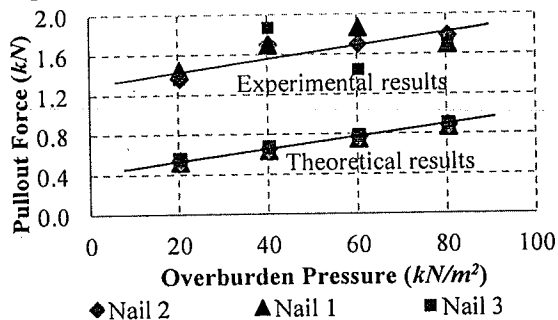


Fig.4: Variation of Peak Pullout Force with Overburden Pressure

#### 3.2 Effect of Degree of Saturation on Pullout Resistance

In order to study the effect of soil saturation on pullout resistance, pullout tests were conducted for overburden pressure of  $60 \text{ kN/m}^2$  under two saturation conditions and results are presented in Table 2.

Table 2 Pullout Forces under two Saturation Conditions

Degree of Saturation (%)	Pullout Force (kN)		
	Nail 1	Nail 2	Nail 3
84	1.87	1.70	1.44
93	1.44	1.36	1.28

It can be observed that with the increase of degree of saturation, pullout force gradually decreases. This is mainly due to reduction of shear strength parameters over soil saturation. This is a clear indication that during the design of soil-nails, it is important to use residual shear strength parameters rather than peak shear strength parameters to calculate the pullout resistance.

#### 3.3 Effect of Cement Grout on Pullout Resistance

In soil-nail stabilized slopes, generally nails are placed in concrete/cement grouted holes. Therefore, the most influencing factor on soil-nail pullout resistance is soil-grout interface. The pullout force over overburden pressure on soil-grout interface is shown in Figure 5. It can be noticed that the pullout resistance of soil-grout interface significantly higher than that of soil-nail interface. The pullout resistance under soil-grout interface is 4.8-6.0 times higher than that of soil-nail interface. This clearly shows that the effectiveness of the use of proper grouting in soil-nailing system.

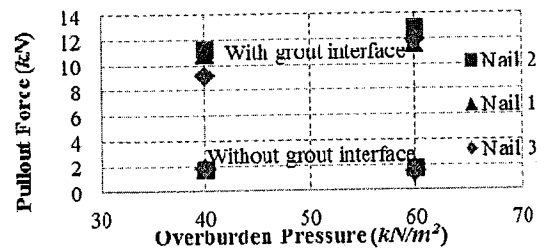


Fig.1: Effect of Cement Grout on Pullout Resistance

#### 3.4 Comparison of Numerical Results with Experimental Results.

The variation of shear stress along the nail during pullout is shown in Figure 6. Based on the Figure 6, point of maximum shear stress, active zone and passive zone within the nail can be clearly identified. The failure plane was generated by connecting the points of maximum shear stress and thereby

the inclination of the failure plane was determined. The variation of distance to the point of maximum stress from the face of the slope with depth is illustrated in Figure 7. Hence, the inclination of the failure plane can be identified as  $65^\circ$  to the horizontal. The theoretical inclination of failure plane in a passive zone is taken as  $45^\circ + (\phi/2)$ , which is  $59^\circ$  for this lateritic soil. Therefore the resulted failure plane is reasonable, although the generation of this failure surface was done by three points which would not be much accurate.

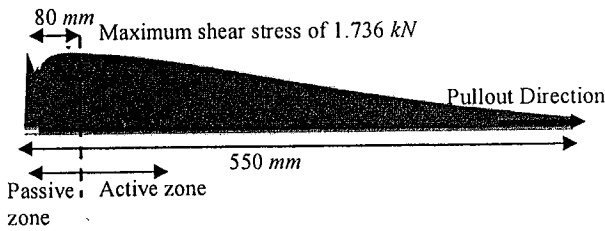


Fig. 6: Shear Stress Variation along the Soil-Nail Interface

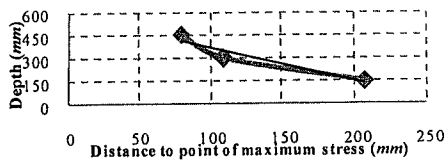


Fig 7: Failure Plane Analysis

Further, soil deformation due to nail pullout based on numerical analysis is presented in Figure 8. It can be observed that a relatively higher soil deformation occurred close to nail 2 during pullout of nail 1. As such, peak pullout resistance of nail 2 is less than that of nail 1 (Figure 3) even though nail 2 is subjected to higher effective vertical stress than that of nail 1. This is a clear indication of the influence one nail on pullout resistance of another. The pullout force values at different overburden pressures under both experimental and numerical analysis are presented in Figure 9. It can be seen that both methods depict similar results. Since these numerical results and experimental results are almost equal, the range of 2.0 – 2.7 for multiplication factor that was introduced in Equation 2 can be validated.

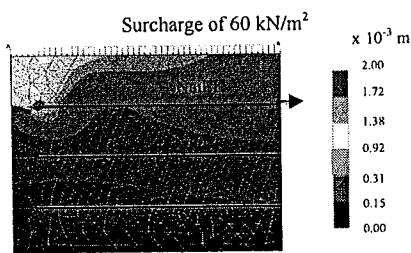


Fig 8: Soil Deformation with the Pullout of Nail 1

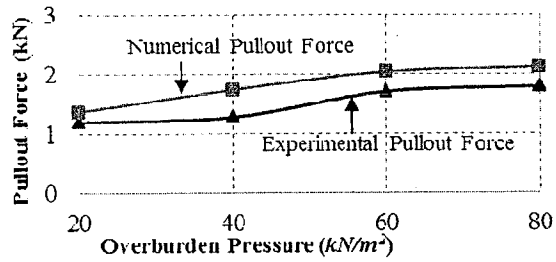


Fig 9: Comparison of Experimental and Numerical Results

#### 4. CONCLUSIONS

From the test results it can be concluded that the pullout force increases with the increase of overburden pressure and therefore, the fill height up to the nail interface and the externally applying surcharge need to be co-related in the design of soil-nail structures. Also pullout force decreases with the increase of degree of saturation due to the lower shear strength in wet soil and it is a clear indication that it is important to use residual shear strength parameters rather than peak shear strength parameters to calculate the pullout resistance during the design of soil-nail structures.

It is clear that the field pullout force values are considerably higher compared to the theoretical pullout force values calculated based on Equation 1 and therefore multiplication factor of 2 – 2.7 can be introduced to the theoretical values in order to be equal with the field values for a soil-nail interface. These values can be incorporated in soil-nail designs to make them cost effective.

Furthermore, it shows that the grout interface properties (shear strength parameters) is the most influencing factor for the pullout resistance of a soil nail and it causes for a significant increase of pullout force by making a strong bonding between the nail and the surrounding soil. Grout injection to the soil has caused for filling of voids in the surrounding soil and hardened to enhance the bonding.

#### REFERECES

Junaideen, S. M., Tham, L. G., Law, K. T., Lee, C. F. and Yue, Z. Q., 2004. 'Laboratory study of soil nail interaction in loose, completely decomposed granite', *Canadian Geotechnical Journal*, 274-286.

Meetananda, D. C. A., Premarathne, B. D. H. and Priyantha, H. M. S., 2001, 'The use of soil nailing technique in stabilizing slopes', Final year research project, Dept. of Civil Engineering, University of Moratuwa.

Milligan, G. W. and Tei, K., 1998, 'The pullout resistance of model soil nails', *Soils and Foundations* 38(2), 179-190.

Powell, G. E., and Watkins, A. T., 1992, 'Soil nailing to existing slopes as landslide preventive works', *Hong Kong Eng.*, 20, March, 20-27.

Pradhan, B., Tham, L. G., Yue, Z. Q., Junaideen, S. M. & Lee, C. F., 2006, 'Soil-nail pullout interaction in loose fill materials', *International Journal of Geomechanics*, 238-247.



# Experimental Investigation on Strength and Deformation Characteristics of Crushed Concrete Aggregate

R. K. S. R. Ratnayake

Department of Civil Engineering, University of Moratuwa, Sri Lanka

**ABSTRACT:** Currently world is concerned about the construction and demolition waste as they have a significant effect on environment and economy. One of the major construction and demolition waste is scrap concrete and it can be recycled and reuse for several purposes. This study focus on strength and deformation characteristics of crushed concrete and its potential for geotechnical backfill applications. Study was done with series of CD tri axial tests and found that the friction angle ( $\phi'$ ) is  $32^\circ$  and cohesion ( $C'$ ) is  $130 \text{ kN/m}^2$ . Also it is found that the maximum dry density is  $1850 \text{ kg/m}^3$  at optimum moisture content of 13% and California bearing ratio (CBR) is 118.6. Concluding, experiments shows that CC has considerable shear strength characteristics which makes them a potential backfill material in terms of strength and deformation characteristics of CC.

## 1 INTRODUCTION

### 1.1 General

Most common waste produced in construction and demolition site is CC. CC is made out of construction and demolition waste generated from construction sites. After sieving and proper grading they can be used as coarse aggregate for concrete or paving or non-paving applications. CC contains particles off all size from fine to coarse.

There are several advantaged of CC as a fill material, such as, reduce the environmental problem arise due to the extensive quarrying activities, reduce the amount of landfill and respective environmental impact such as high temperature rise and problems related to transportation of scrap concrete out of the sites and cost reduction for transportation when there is no local landfill is available. Also recycled concrete products have a carbon footprint 65% less than equivalent quarry products (WBCSD (2009))

However, before use these scrap concrete it is essential to evaluate the suitability the crushed material with a great care.

### 1.2 Important findings from literature survey

As Rathje et al. (2003) indicated, "An ideal select backfill material should exhibit high drained shear strength parameters ( $c'$  and  $\phi'$ ) and have good drainage properties. To avoid excessive surface deformations, the selected backfill should also exhibit low compressibility over time"

And again according to the results obtained from Rathje et al. (2006) crushed concrete has shear

strength characteristics compatible as those of conventional fill materials. The determined effective shear strength parameters for crushed concrete aggregate from triaxial tests are as follows,

Table 1. Shear strength parameters

Parameter	From experiment	TxDOT specification
Cohesion	$152 \text{ kN/m}^2$	$160 \text{ kN/m}^2$
Friction angle	$46^\circ$	$46^\circ$

Also, past studies shows that the gradation of CC aggregates are either well graded sand or well graded gravel.

According to the Rathje et al. (2006) from the compaction curve for CC, the dry unit weight increases when the moisture content increases up to about 12% and after dry unit weight remains relatively constant as the specimen gets saturated and specimen cannot be prepared at higher water contents greater than 14% because excess water starts to drain out from the mould.

In order to find the bearing capacity of CC Aurstad et al. (2006) have carried out CBR tests and the results from their shows CBR values for test fraction 0 – 19mm as 120 - 130. Hence, they have shown that the CC has good bearing capacity.

According to both Lim et al. (2001) and Rathje et al. (2006) specific gravity and water absorption is different compared to the traditional backfill material due to the presence of cement in mortar. Rathje et al. (2006) has identified that the specific gravity of CC is in the range of 2.0 – 2.5 and the

water absorption of CC is in the range of 2-8 % depending on their particle size. And it also mentioned that this low specific gravity is caused by finer mortar particles in the CC.

*Main objective of this research is to identify the suitability of CC as a fill material by determine the strength and deformation characteristics of CC with a series of triaxial tests.*

## 2 METHODOLOGY

The experimental program carried out in the current study is detailed in this section. All the experimental works were conducted according to the ASTM standards.

### 2.1 Sample preparation

Early researchers have found that the effect of compressive strength of original concrete has fairly no effects on the characteristics of crushed concrete aggregate such as stiffness and strength after it is crushed and used as a backfill material (Tatsuoka et al. (2013)).

Hence, concrete cubes used for testing were used to prepare the samples. They were crushed so that the maximum particle size is 19mm as shown in Fig. 1 and samples were prepared according to the ASTM: D75



Fig. 1 Preparation of CC sample

### 2.2 Finding index properties of CC

#### 2.2.1 Sieve analysis

Sieve analysis was done according to the ASTM C136. A sample of oven dried aggregates of 1000g in mass is separated through a series of sieves of openings in order of decreasing from top to bottom and determined the particle-size distribution.

#### 2.2.2 Laboratory Compaction

Amount of material retained on 5mm sieve is 28 % which is greater than 7%, hence as mentioned in the ASTM standards, method C have been adopted in conducting the proctor compaction test.

This was done according to the ASTM D 1557. When the test was done for an air dried sample it

was very difficult to control the small moisture content (m.c.) due to higher water absorption nature of CC. Hence again the test was conducted to the oven dried sample to obtain dry densities at lower m.c.

### 2.2.3 California Bearing Ratio test

ASTM D 1883 was practiced for this test. Three specimens were prepared to the optimum moisture content (M.C. = 13%) by compacting to three different compaction efforts as 60, 56 and 30 blows per layer.

They were cured in a water tank for 96 hours and then each specimen was subjected to penetration by a cylindrical rod while taking the results of both penetration and respective load.

Finally CBR values were determined by plotting the stress vs. penetration depth graph. CBR versus dry unit weight graph was plotted in order to find the CBR at specific dry density.

### 2.3 Shear strength and deformation characteristic of CC

Series of Consolidated-Drained Triaxial tests were conducted according to the ASTM D 7181.

#### 2.3.1 Specimen preparation of triaxial test

Specimens were prepared as remolded samples, and particles larger than 10mm were removed as a large scale tri axial apparatus is not available at the laboratory. However, as it is mentioned by Tatsuoka et al. (2013) when compacted to the same dry density, original CC with larger particles exhibits significantly higher strength and stiffness than the sample where larger particles are removed. Therefore our purpose, which is identifying the potential use of CC as a fill material can be satisfactorily done with this test.

The adequate water content was added to the weighted sample, so that the specimen is compacted to its maximum dry density and made sure the sample does not collapse or disturbed when the sampler is removed.

#### 2.3.2 Procedure of testing

With the prepared sample encased in rubber membrane triaxial chamber is assembled and axial load piston is brought to the top cap. Then the chamber was filled with the confining fluid, water and was placed on the axial loading device.

Before the cell pressure is applied, sample was left for adequate time to saturate. Pore pressure was measured right after the cell pressure is applied as it indicates whether the specimen is fully saturated or not. Once the pore pressure is dissipated axial load is applied at a slow rate (0.125 mm/min) so that the pore water pressure inside the specimen is negligible. During measuring axial deformations frequent readings were taken to capture the initial stiff part of the curve.



### 3 TEST RESULTS AND EVALUATION

#### 3.1. Dry Sieve Analysis

Dry sieving was done for both air dried and oven dried samples and determined the gradation of CC. The material was classified according to the Unified Classification system of Soil (UCSS). Particle size distribution is shown in the Fig. 2

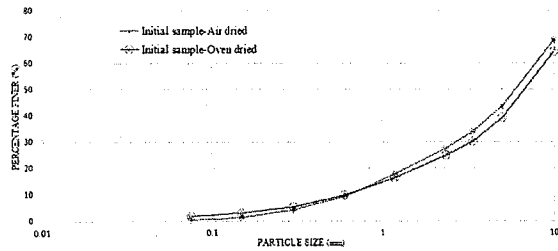


Fig. 2 Particle size distribution of CC

According to UCSS finer percentage is considerably low (less than 5%) Hence it is assumed that no influence from fines and classified as a *Well graded sand*

#### 3.2. Modified proctor compaction test

Maximum particle size was 19mm, hence proctor compaction test was done with modified effort.

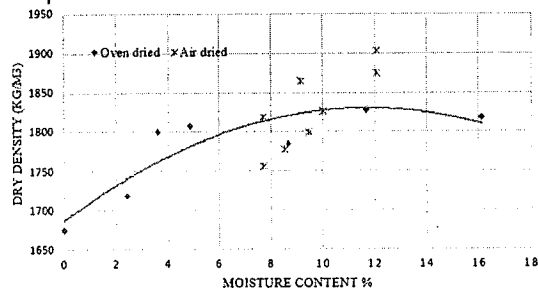


Fig. 3 Modified proctor compaction curve

From the Fig. 3 maximum dry density is found as 1850 kg/m<sup>3</sup> while optimum moisture content is 13%. After proctor compaction was done, sieve analysis was conducted to see whether particle breakage has taken place. Particle size distribution is shown in Fig. 4

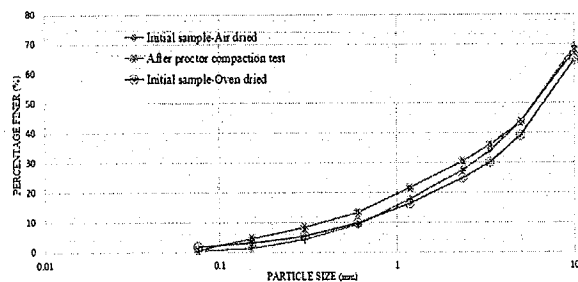


Fig. 4 Particle size distribution after compaction test

There is a small variation in particle size distribution after the compaction, but it is not significant. Hence it can be noted that there is no significant particle breakage during compaction.

#### 3.3. California Bearing Ratio Test (CBR)

CBR test was conducted for different compaction levels as 30, 56 and 60 blows per layer and plotted the load- penetration curves. Then the results were determined while correcting the error due to surface irregularities. Obtained results are shown in Table 1

Table 2. CBR test results

No of bows per layer	Dry Density (kg/m <sup>3</sup> )	CBR value
30	1788	78.0
56	1831	138.8
60	1877	38.9

CBR values at any desired dry density can be found out with the dry density versus CBR graph shown below.

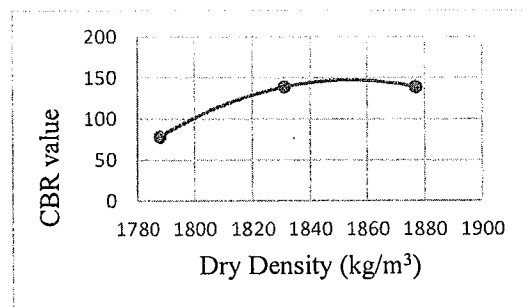


Fig. 5 CBR vs. Dry density graph

#### 3.4. Consolidated Drained Triaxial test

Three strain controlled, consolidated triaxial tests were performed for three different confining pressures at 50, 100 and 150 kPa

Axial strain vs. Deviator stress graphs were plotted and the maximum deviator stress and the corresponding axial strain was obtained from Fig. 6

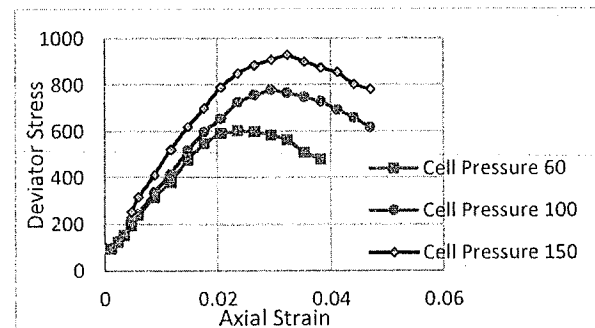


Fig. 6 Deviator stress vs. Axial strain graph

Failure was defined at maximum principal stress and Mohr circles were drawn using calculated major and minor principal stresses at failure. Then the Mohr Coulomb failure envelope was developed as shown in the Fig. 7

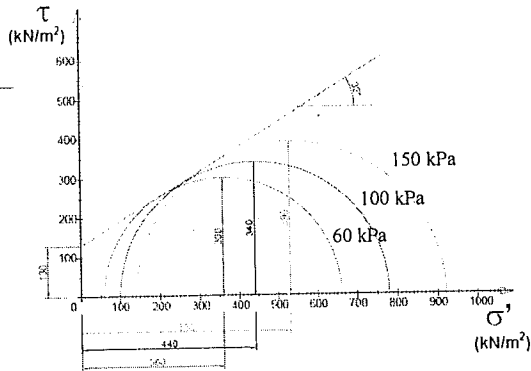


Fig. 7 Mohr-Coulomb failure envelop

Failure plane couldn't be identified clearly but from the envelop shear strength parameters can be determined.

Table 3 Shear strength parameters of CC

Shear strength parameter	Value from Mohr-Coulomb envelop
Cohesion	130 kPa
Friction angle	32°

### 3.5. Summary of Test results

Test results are summarized in the Table-3

Table 4 Summary of test results

Characteristics of CC	Test results
Soil classification	Well graded sand
Maximum dry density	1850 kg/m <sup>3</sup>
Optimum moisture content	13%
Cohesion	130 kPa
Friction angle	32°
CBR	118.6

As it can be clearly seen, even though there is very small fine content, cohesion is a higher value. This may be due to the presence of mortar. Tatsuoka et al. (2013) stated that "High strength and stiffness of well-compacted CCA are due to not only a high coefficient of uniformity and a relatively angular particle shape, but also rather stable inter-particle contacts resulting from relatively soft and weak mortar layers covering stiff and strong core particles".

## 4 CONCLUSION

In general, index properties of CC obtained from the sieve analysis, proctor compaction test and bearing

capacity of obtained from CBR test indicate that, CC is a compatible alternate backfill material.

Also, shear strength parameters determined using strain controlled consolidated drained triaxial test exhibits high friction angle, i.e.  $\phi' = 32^\circ$

Hence, it can be concluded that CC is a potential alternative backfill material in terms of strength and deformation characteristics of CC.

However, there was a clear difference between air dried and oven dried CC samples, where oven dried samples exhibits distinct, hardened crust of material which shows clog-mentation of cement particles in the sample. This dehydration of cement may increase the strength to some extent after compaction with time (Rathje et al. (2006))

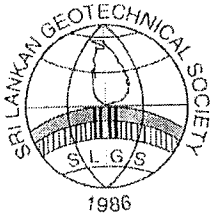
Hence, it is advisable to study both this aging effect of compacted CC and effect of age of original concrete in further studies.

## ACKNOWLEDGMENTS

I would like to express my deepest gratitude to Dr. L. I. N. De Silva, research supervisor and everyone who guided and supported to complete this project successfully.

## REFERENCES

- Aurstad, J., Aksnes, J., Dahlhaug, J. E., Berntsen, G., & Uthus, N. (2006). Unbound crushed concrete in high volume roads— A field and laboratory study. In 5th International Conference on Research and Practical Applications Using Wastes and Secondary Materials in Pavement Engineering
- Goodwin, I. C. A., & Laycock, E. A. (2004, September). Shear behavior of crushed concrete and bricks. In Sustainable Waste Management and Recycling: Construction Demolition Waste: Proceedings of the International Conference Organized by the Concrete and Masonry Research Group and Held at Kingston University-London on 14-15 September 2004 (p. 205). Thomas Telford.
- Lim, S., Kestner, D., Zollinger, D. G., & Fowler, D. W. (2003). Characterization of crushed concrete materials for paving and non-paving applications (No. TX-04/7-4954-1.)
- Rathje, E., Trejo, D. & Folliard, K. (2003). Potential use of crushed concrete and recycled asphalt pavement as backfill for mechanically stabilized earth walls (NO. FHWA/TX-06/0-4177-S)
- Rathje, E. M., Rauch, A. F., Trejo, D., Folliard, K. J., Viyanant, C., Esfellar, M., & Ogalla, M. (2006). Evaluation of crushed concrete and recycled asphalt pavement as backfill for mechanically stabilized earth walls (No. FHWA/TX-06/0-4177-3)
- Recycling Concrete (2009, June). The Cement Sustainability Initiative. Washington D.C, United States: The World Business Council for Sustainable Development (WBCSD)
- Touahamia, M., Sivakumar, V., & McKelvey, D. (2002). Shear strength of reinforced-recycled material. Construction and Building Materials, 16(6), 331-339
- Tatsuoka, F., Tomita, Y. I., Iguchi, Y., & Hirakawa, D. (2013). Strength and stiffness of compacted crushed concrete aggregate. Soils and Foundations, 53(6), 835-852



# Determination of Age of Municipal Solid Waste Through Soil Tests

J. Thirojan

*Department of Civil Engineering, University of Moratuwa, Sri Lanka*

**ABSTRACT:** The evaluation of the geotechnical properties of MSW is difficult due to heterogeneity nature and the changes in such properties due to degradation. Therefore, the variation of geotechnical properties of MSW with fill age has to be studied. MSW with known age were collected from Kallundai and Karadiyana dump sites. The particle size distribution, specific gravity, Atterberg limit, proctor compaction, permeability and direct shear tests were conducted on nine samples in order to obtain the variation of geotechnical properties with age of MSW. The particle sizes, gravel percentage, liquid limit, plastic limit, plasticity index, optimum moisture content, hydraulic conductivity and friction angle show decreasing trend, while sand percentage, silt and clay percentage, specific gravity, maximum dry density, waste homogeneity and cohesion show increasing trend with fill age. Some of the data were obtained from published literatures in order to compare the results of the current study. This paper highlights the need to do the changes in the geotechnical properties of MSW with fill age when designing.

## 1 INTRODUCTION

The most of the dump sites in Sri Lanka were located in the city centers, and some of them have been abandoned due to public pressure due to environmental issues and some of them had even reached their design capacities. Due to the rapid growth of population in major cities like Colombo, Kandy and Jaffna, rapid development and urbanization caused scarcity of lands available for new constructions. Therefore, the abandoned and design capacity reached dump sites can be used for new constructions for further development of a city. As the dumped wastes become soil, it can be used as a fill material for construction activities and this would be economical.

Nowadays there is an increasing tendency in the world to construct buildings on the design capacity reached landfills. Almost all of the landfill embankments were built with the municipal solid wastes of several decades. As the municipal solid wastes consist of high organic matters, it will undergo for several phases of degradation [Chen et al (2009), Zhan et al (2008), Reddy et al (2009), Haque (2007)]. Due to these changes and heterogeneity nature, the geotechnical properties of MSW show a tendency to vary with the age of fill. Therefore, it is important to consider the variation of geotechnical properties of MSW with respect to age of fill in order to study the adverse effects of dump site lands such as settlement, slope instability and shear failure, when constructing on the design capacity reached landfills.

Municipal solid waste (MSW), commonly known as trash or garbage is the household waste, which typically consists of food and garden wastes, paper products, plastics, rubber, textiles, wood, ashes, and soils [Dixon and Langer (2006), Chen et al (2009)]. These components are different in size, shape, compressibility, tensile strength and degradability [Chen et al (2009)]. The composition of MSW generally varies from country to country, region to region and period to period. Even within a particular landfill with similar MSW input, the composition of MSW varies with its fill age due to the degradation process of organic matter. The composition of the waste, moisture content, organic matter content, permeability, particle size distribution, and specific gravity are important MSW characteristics. These parameters greatly influence the geotechnical characteristics of the waste. Therefore, there is a need to understand the MSW characteristics with decomposition.

In this research, an attempt was made to find the relationship between some geotechnical properties of MSW and the fill age of MSW. For that purpose Kallundai dump site in Jaffna and Karadiyana dump site in Colombo were selected to collect the samples.

## 2 OBJECTIVES AND METHODOLOGY

The purpose of this study is to identify the importance of age of MSW with respect to geotechnical properties of MSW through soil tests. The following procedure was adopted.

1. Identifying the geotechnical properties of MSW by performing the following tests: Particle size distribution tests, specific gravity tests, Atterberg limit tests, Proctor compaction tests, permeability tests and direct shear tests
2. Analyzing the experimental results with available records from literature.

### 3 EXPERIMENTAL WORKS

A series of experiments were conducted according to the guidelines such as BS1377 and ASTM volume 04.08 in order to meet the objectives of this research study. All the experiments were done on the municipal solid wastes samples with known age in order to identify the variation of geotechnical properties of MSW with fill age.

Seven samples from Kallundai dump site (age in years <5, 5-7, 7-10, 10-13, 13-15, 15< and 5-7 burnt), two samples from Karadiyana (1 and 2 years), and one sample from Matara (1-3 years) were used in the experiments.

### 4 RESULTS AND DISCUSSION

#### 4.1 Particle size distribution test

The results of combined sieve & hydrometer analysis of oven dried samples are provided in Fig 1. The variation of  $D_{60}$ ,  $D_{30}$ , and  $D_{10}$  were shown in Fig 2, in which  $D_{60}$  significantly decreasing,  $D_{30}$  slightly decreasing and  $D_{10}$  shows no significant variation with fill age. The variation of  $C_c$  and  $C_u$  were shown in Fig 3, in which  $C_u$  significantly decreasing while  $C_c$  shows no significant variation with fill age. The variation of percentages of MSW soil components were shown in Fig 4, in which percentage of gravel decreasing while percentage of sand and percentage of silt & clay increasing with fill age of MSW.

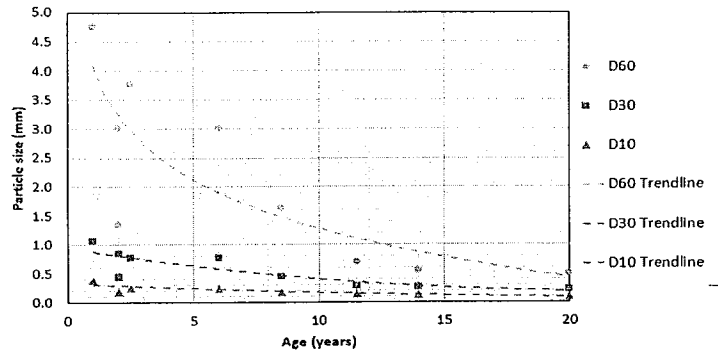


Fig 2 Variation of  $D_{60}$ ,  $D_{30}$  and  $D_{10}$  with age of MSW

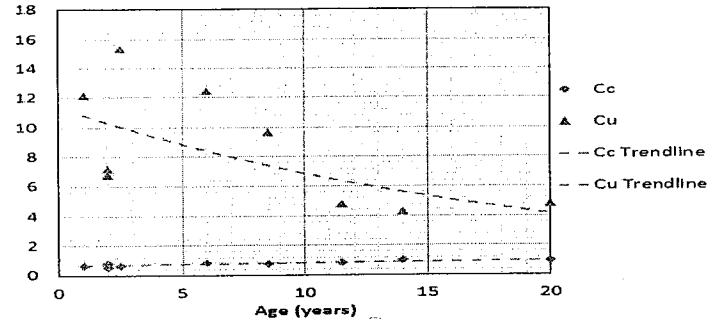


Fig 3 Variation of  $C_c$ , and  $C_u$  with age of MSW

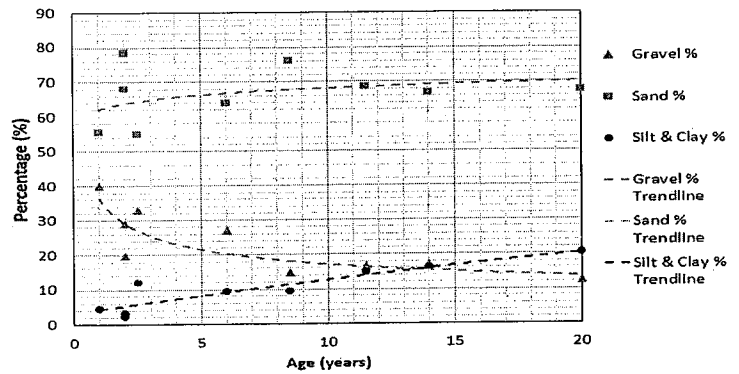


Fig 4 Variation of percentage of soil components with age of MSW

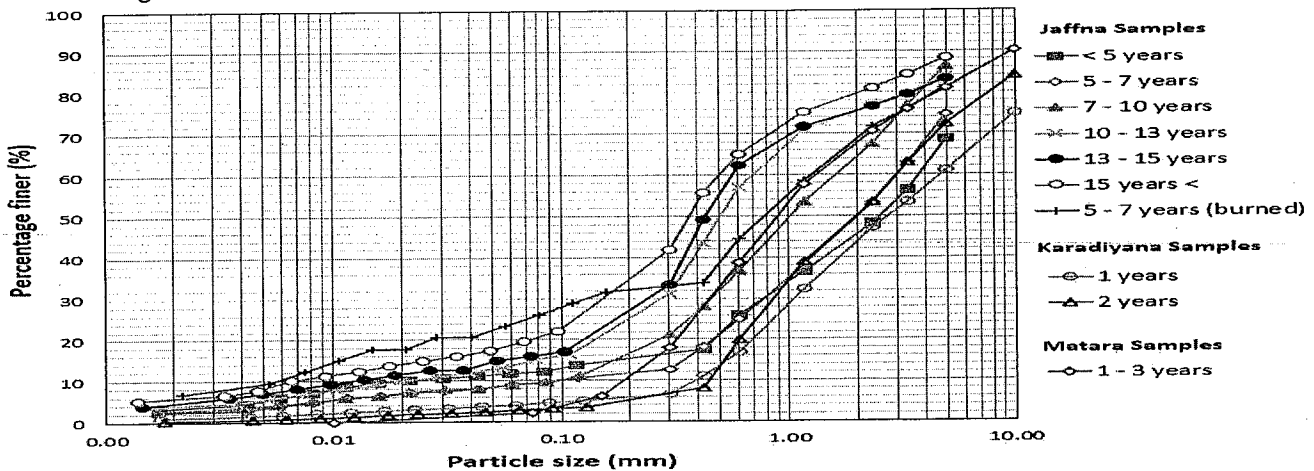


Fig 1 Particle size distribution of tested MSW samples

### 4.2 Specific gravity test

The comparison of specific gravity of MSW of current study with literatures was shown in Fig 5, in which specific gravity shows an increasing tendency

with fill age. The increase in specific gravity is mainly attributed to less organic matter content, which could be due to completion of biodegradation of MSW with fill age.

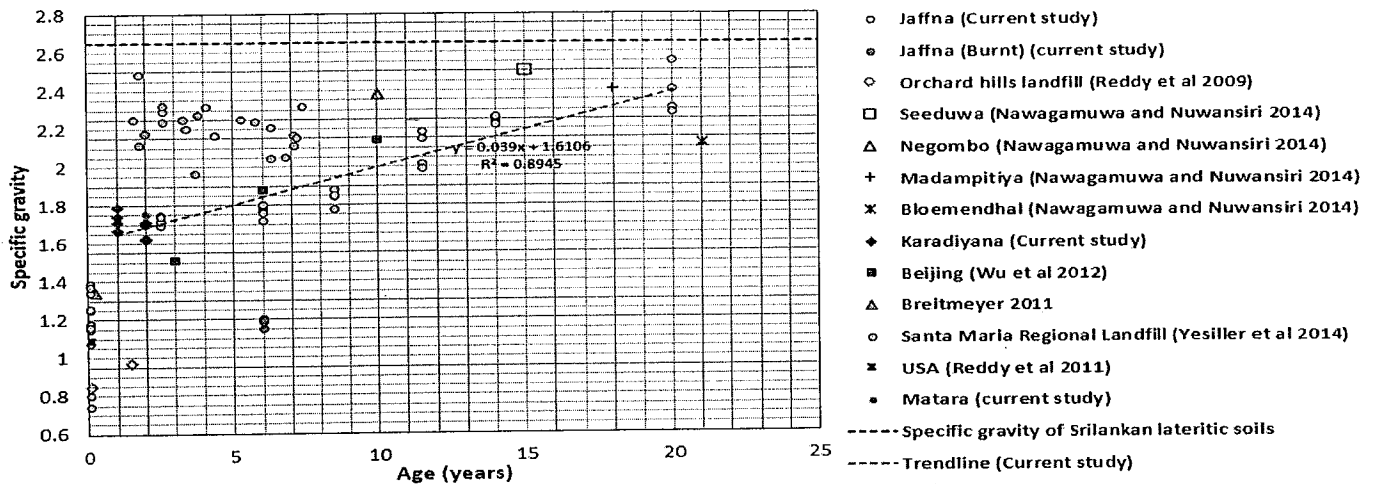


Fig 5 Comparison of specific gravity of MSW with reported literatures

### 4.3 Atterberg limits test

The variation of Atterberg limits of MSW samples were shown Fig 6, in which Atterberg limits shows decreasing tendency with fill age of MSW. The decrease in Atterberg limits was attributed to the mixing of cover soil with MSW.

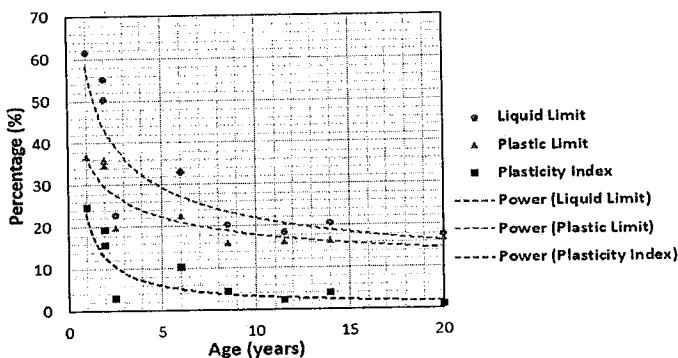


Fig 6 Variation of Atterberg limits with age of MSW

### 4.4 Proctor compaction test

The variation of optimum moisture content (OMC) and maximum dry density (MDD) of MSW samples were shown in Fig 7, in which OMC shows decreasing tendency, while MDD shows an increasing tendency with fill age of MSW. The increase in MDD may be due to the increase in the finer particles with fill age of MSW. This is already observed in Specific Gravity relationship too.

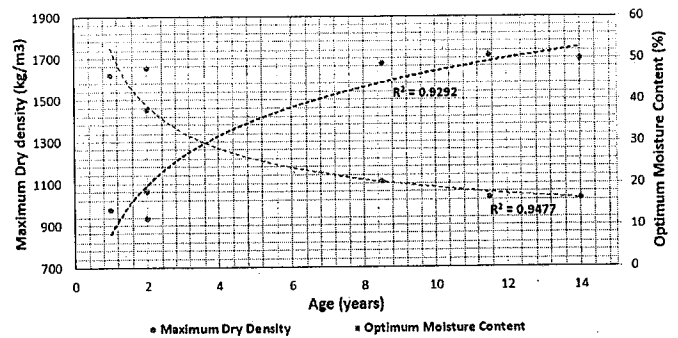


Fig 7 Variation of optimum moisture content and maximum dry density with age of MSW

### 4.5 Permeability test

The variation of hydraulic conductivity of MSW samples were shown in Fig 8, in which hydraulic conductivity of MSW shows decreasing tendency with fill age of MSW. The decrease in hydraulic conductivity with fill age of MSW can be attributed to reduction of particle size with degradation, the increased percentage of fines, and resulting higher density.

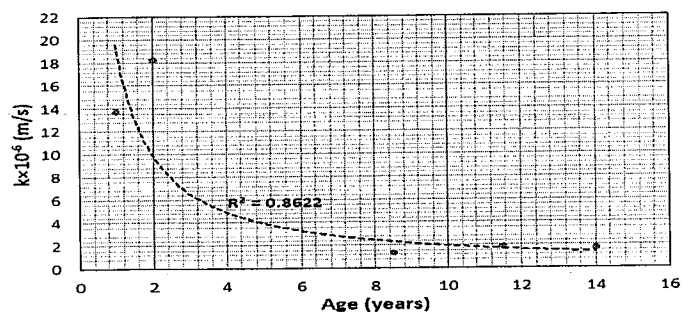


Fig 8 Variation of hydraulic conductivity with age of MSW

4.6 Direct shear test

The variation of cohesion of MSW samples were shown in Fig 9, in which cohesion shows an increasing tendency with fill age of MSW. The variation of angle of friction of MSW samples were shown in Fig 10, in which angle of friction shows decreasing tendency with fill age of MSW. The changes in cohesion and angle of friction can be attributed to the composition changes in fiber and plastic materials. The fiber content such as textiles,

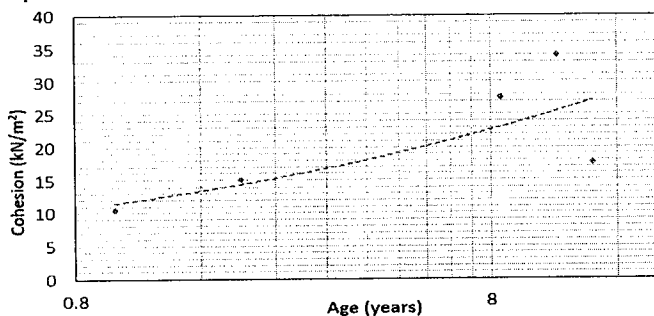


Fig 9 Variation of cohesion with age of MSW

wood leather, etc and the plastics content decreased with the fill age. The decreasing trend of these contents is due to the change in MSW composition. The fiber and plastic materials generally pose a low friction resistance and hence lead to a low mobilized friction angle. The fiber and plastic materials provide reinforcement effect and hence lead to a high mobilized cohesion.

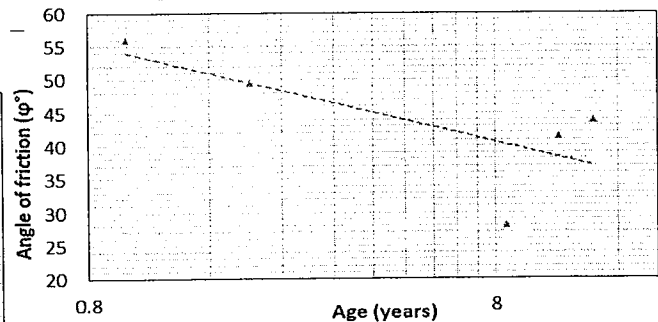


Fig 10 Variation of angle of friction with age of MSW

The analysis results of conducted experiments were summarized in Table 1.

Table 1 - Summary of results obtained from conducted experiments

MSW sample	Age (years)	Specific gravity	Liquid limit (%)	Plastic limit (%)	OMC (%)	MDD (kg/m³)	Hydraulic conductivity (m/s)	Cohesion (kN/m²)	Angle of friction
Jaffna 1	< 5	1.7247	22.85	19.89	-	-	-	-	-
Jaffna 2	5 - 7	1.7652	32.97	22.55	-	-	-	-	-
Jaffna 3	7 - 10	1.8368	20.42	15.90	20.34	1673.99	1.333×10 <sup>-6</sup>	27.6	28
Jaffna 4	10 - 13	2.0814	18.48	16.14	16.70	1714.22	1.905×10 <sup>-6</sup>	33.97	41.49
Jaffna 5	13 - 15	2.2392	20.52	16.47	16.47	1696	1.714×10 <sup>-6</sup>	17.65	43.87
Jaffna 6	15 <	2.3822	17.69	16.63	-	-	-	-	-
Jaffna 7	5 - 7	1.1818	-	-	-	-	-	-	-
Karadiyana 1	1	1.7285	61.68	36.84	46.01	978.61	1.37×10 <sup>-5</sup>	10.46	56
Karadiyana 2	2	1.6632	50.24	34.63	47.65	933	1.823×10 <sup>-5</sup>	15.07	49.47
Matara 1	1 - 3	1.7521	55.32	36.05	37.68	1062.99	-	-	-

5 CONCLUSIONS

Variation of geotechnical properties of MSW with fill age is presented in this study.

Particle size distribution tests have shown that particle size decreases, hence waste homogeneity increases with fill age.

Specific gravity of MSW increases (1.66 to 2.38) with fill age as organic matter decreases due to biodegradation.

Atterberg limit tests have shown that liquid limit (61% to 17%), plastic limit (36% to 15%), and plasticity index decreases with fill age. This variation is due to the mixing of cover soil with MSW.

Proctor compaction tests have shown that optimum moisture content decreases (47% to 16%) as porous material content decreases due to degradation, while maximum dry density increases

(933kg/m<sup>3</sup> to 1714kg/m<sup>3</sup>) as finer particles increases with fill age.

Permeability tests have shown that hydraulic conductivity decreases (1.8×10<sup>-5</sup> m/s to 1.3×10<sup>-6</sup> m/s), hence water retention increases with fill age. This is due to reduction of particle sizes with degradation, increased percentages of fines and resulting higher density.

Direct shear tests have shown that cohesion increases (10 kN/m<sup>2</sup> to 33 kN/m<sup>2</sup>), while angle of friction decreases (56° to 28°) with fill age. This variation is due to composition changes in fiber and plastic materials with fill age.

ACKNOWLEDGMENTS

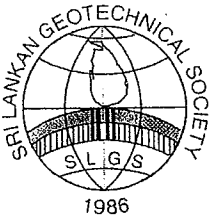
The staff members of the Soil Mechanics Laboratory of Department of Civil engineering, University of Moratuwa and officials of relevant municipal councils are kindly acknowledged for their support.

## REFERENCES

- ASTM D 422, (1963). Standard test method for particle size analysis of soils. Annual book of ASTM standards. American Society for Testing and Materials, West Conshohocken, PA.
- ASTM D 698, (1978). Standard test method for moisture-density relations of soils and soil-aggregate mixtures using 5.5-lb (2.49-kg) rammer and 12-in (305-mm) drop. Annual book of ASTM standards. American Society for Testing and Materials, West Conshohocken, PA.
- ASTM D 854, (1983). Standard test method for specific gravity of soils. Annual book of ASTM standards. American Society for Testing and Materials, West Conshohocken, PA.
- ASTM D 2434, (1968). Standard test method for permeability of granular soils (constant head). Annual book of ASTM standards. American Society for Testing and Materials, West Conshohocken, PA.
- ASTM D 3080, (1972). Standard test method for direct shear test of soils under consolidated drained conditions. Annual book of ASTM standards. American Society for Testing and Materials, West Conshohocken, PA.
- ASTM D 4318, (1983). Standard test method for liquid limit, plastic limit and plasticity index of soils. Annual book of ASTM standards. American Society for Testing and Materials, West Conshohocken, PA.
- Breitmeyer R.J, (2011). Hydraulic characterization of municipal solid waste. Ph.D. dissertation, University of Wisconsin, Madison, WI.
- BS1377, (1990). Methods of test for soils for civil engineering purposes. British Standards.
- Chen Y.M, Zhan T.L, Wei H.Y, and Ke H, (2009). Aging and compressibility of municipal solid wastes. *Waste Management*, 29:86-95
- Dixon N., Russell D., & Jones V, (2005). Engineering properties of municipal solid waste. *Geotextiles and Geomembranes* 23:205-233
- Gomes, C., Lopes, M. L., & Oliveira, P. J. (2013). Municipal solid waste shear strength parameters defined through laboratory and in situ tests. *Journal of the Air & Waste Management Association*, 63(11):1352-1368
- Haque, M. A. (2007). Dynamic characteristics and stability analysis of municipal solid waste in bioreactor landfills. Phd Thesis. Faculty of the Graduate School, University of Texas, Arlington.
- Karimpour-Fard, M., Machado, S. L., Shariatmadari, N., & Noorzad, A. (2011). A laboratory study on the MSW mechanical behavior in triaxial apparatus. *Waste Management*, 31:1807-1819
- Karimpour-Fard, M., Shariatmadari, N., Keramati, M., & Kalarijani, H. J. (2014). An experimental investigation on the mechanical behavior of MSW. *International Journal of Civil Engineering, Geotechnical Engineering*, 292-303
- Machado, S. L., Karimpour-Fard, M., Carvalho, M. F., Vilar, O. M., & Santos, A. C. (2014). MSW characteristics and landfill performance in tropical regions. *International Journal of Civil Engineering, Geotechnical Engineering*, 238-250
- Machado, S. L., Karimpour-Fard, M., Shariatmadari, N., Carvalho, M. F., & Nascimento, J. C. (2010). Evaluation of the geotechnical properties of MSW in two Brazilian landfills. *Waste Management*, 30:2579-2591
- Nawagamuwa, U. P., & Muhilan, K. (2015). Long term settlement behaviour of dump wastes in Sri Lanka, Case study on Bloemendhal dump site. *Proceedings of the International Symposium on Advances in Civil and Environmental Engineering Practices for Sustainable Development (ACEPS-2015)*, Galle, Sri Lanka. March 2015.
- Nawagamuwa U.P, and Nuwansiri R.W, (2014). Compaction characteristics of municipal solid wastes at open dumpsites in Sri Lanka. *Proceedings of Geo-Shanghai 2014 International Conference*, May 26-28, 2014. Shanghai, China. (pp 110 - 119).
- Nawagamuwa, U. P., Gunaratne, W. D., Kirubajiny, P., Thiviya, T., & Priyadarshana, H. K. (2013). Study on the geotechnical properties of open dumps in Sri Lanka. *Proceedings of ICSECM 2013*.
- Nawagamuwa, U. P., Rajeevan, R., & Tharanga, W. U. (2015). Study on the strength characteristics of MSW in Sri Lanka. *Asian Regional Conference on Soil Mechanics and Geotechnical Engineering*. Fukuoka, Japan.
- Pandey, R. K., & Tiwari, R. P. (2015). Physical characterization and geotechnical properties of municipal solid waste. *IOSR Journal of Mechanical and Civil Engineering*, 15-21
- Pinapati, K. K. (2005). Variation of geotechnical strength properties with age of landfills accepting biosolids. MSc Thesis. Department of Civil and Environmental Engineering, University of Central Florida, Orlando, Florida.
- Reddy K.R, Gangathulasi J, Parakalla N.S, Hettiarachchi H, Bogner J, and Lagier T, (2009). Compressibility and shear strength of municipal solid waste under short-term leachate recirculation operations. *Waste Management and Research*, 27:578-587.
- Reddy K.R, Hettiarachchi H, Gangathulasi J, and Bogner J, (2011). Geotechnical properties of municipal solid waste at different phases of biodegradation. *Waste Management*, 31:2275-2286
- Reddy, K. R., Hettiarachchi, H., Giri, R. K., & Gangathulasi, J. (2015). Effects of degradation on geotechnical properties of municipal solid waste from Orchard Hills landfill, USA. *International Journal of Geosynthetic and Ground Engineering*, 1-24
- Shariatmadari, N., Sadeghpour, A. H., & Mokhtari, M. (2015). Aging effect on physical properties of municipal solid waste at the Kahrizak landfill, Iran. *International Journal of Civil Engineering, Civil Engineering*, 126-136
- Shariatmadari, N., Sadeghpour, A. H., & Razaghian, F. (2014). Effects of aging on shear strength behavior of municipal solid waste. *International Journal of Civil Engineering, Geotechnical Engineering*, 226-237
- Wong, W. W. (2009). Investigation of the geotechnical properties of municipal solid waste as a function of placement conditions. MSc Thesis. Civil and Environmental Engineering, Faculty of California Polytechnic State University, San Luis Obispo
- Wu H, Wang H, Zhao Y, Chen T and Lu W, (2012). Evolution of unsaturated hydraulic properties of municipal solid waste with landfill depth and age. *Waste Management*, 32:463-470
- Yesiller N, Hanson J.L, Cox J.T, and Noce D,E, (2014). Determination of specific gravity of municipal solid waste. *Waste Management*, 34:848-858
- Zekkos, D., Bray, J. D., Kavazanjian, E., Matasovic, N., Rathje, E. M., Riemer, M. F., & Stokoe, K. H. (2006). Unit weight of municipal solid waste. *Journal of Geotechnical and Geoenvironmental Engineering*, 1250-1261
- Zhan, T. L., Chen, Y. M., & Ling, W. A. (2008). Shear strength characterization of municipal solid waste at the Suzhou landfill, China. *Engineering Geology*, 97:97-111







# A Study on the Application of Poker Vibrator for Compacting Quarry Dust

K.H.S.M. Sampath

*Department of Civil Engineering, University of Moratuwa, Sri Lanka*

**ABSTRACT:** Recently as a ground improvement technique, quarry dust is widely used as a filling material to achieve higher bearing strength and to minimize the settlements underneath foundations, especially when the water table is encountered. Practical approaches suggest that a poker vibrator can be used to achieve higher degree of compaction easily, when the ground water table is above the excavation level. However the problem is, currently there is no any proper procedure to follow the filling process and it may diminish the expected results in terms of degree of compaction. Thus it is essential to carry out a sequent of experiments and determine what the optimum methods are, which can be adopted to achieve higher degrees of compaction. Here, the research was basically focused on determining an optimum time of application, preferable layer thicknesses and optimum patterns of applying poker vibrator, in order to achieve acceptable degrees of compaction.

## 1 INTRODUCTION

Improvement of the underlying ground conditions is playing a critical role in the construction process of a foundation. Several techniques are being adopted for the improvement of ground conditions which can be varied due to ground condition and foundation type. Some of the ground improvement techniques adopted in construction field are consolidation and pre-loading, chemical treatment, static and dynamic compaction, etc. (Indraratna and Chu 2005)

One of the major problems that can be aroused in the process is the presence of soil layers which are having low strength parameters. In that case the weak soil layer should be removed up to the required depth and should be filled with a suitable cohesion-less granular soil and compacted well. Then the other major problem is having a higher level of ground water table.

Currently there is a method adopted to overcome those problems in the construction industry, where quarry dust is used as the filling material. Quarry dust with appropriate moisture content and a proper compaction, can achieve a higher degree of compaction as it has rough, sharp and angular particles which lead to a higher DoC due to better interlocking between particles. (Onyelowe, Okafor and Nwachukwu, 2012)

A vibrating technique is the best method to achieve higher degree of compaction in granular soils and quarry dust, rather than a traditional compaction method. (Drnevich, Evans and Prochaska, 2007). In this case a poker vibrator is a better solution which can be used with an appropriate water content to achieve a higher degree of compaction in quarry dust.

However the problem is currently there is no any valid guideline or a procedure to follow this particular process. Also from a literature review it was revealed that there are limited researches done regarding this method of compaction.

In most practical situations this process was done with the experience of the officer in-charge presented at the site. As a result of that it won't be able to achieve the expected degree of compaction in most cases, due to improper guidance or the practice and the lack of knowledge and experience. Therefore it is essential to do a research based on this method and eliminate the improper practice by introducing a proper guideline.

According to a research done by Aziz, Albusoda and Yaseen (2009), this method is more suitable for ground improvements under shallow foundations with circular or rectangular individual footings where the largest dimension is less than around 1.5 m. Thus it is proposed to carry out the experiments in similar containers where the diameter and width are around 1 m.

Also it is proposed to do the experiments under saturated condition as it is impossible to control the moisture content and also it is noticed that in most practical situations, quarry dust is used as filling material when there is a high water table. All these conditions has been taken into consideration when carrying out experiments and always tried to idealize the experiments with the practical situations as much as possible.

Finally, under this research project it is expected to study on the application of poker vibrator for compacting quarry dust by varying different parameters such as layer thickness, application time, different patterns, shape of the container, etc. and find out what the most advisable applications of poker vibrator are, in order to achieve an opti-

imum compaction and through that propose a guidance to optimize the current construction practices.

## 2 RESEARCH OBJECTIVE

After carrying out a series of experiments, the attempt is to propose new guidelines and methods to optimize the current construction practices of application of poker vibrator for the compaction of quarry dust. In order to achieve the above objective, the degree of compaction of quarry dust was measured by varying different parameters such as shape of the container, layer thickness, time of application of poker vibrator and different patterns.

## 3 EXPERIMENT PROGRAMME

### 3.1 Standard Proctor Compaction Test

At the beginning, maximum dry density of the quarry dust sample was determined by carrying out a Standard Proctor Compaction Test according to ASTM D698.

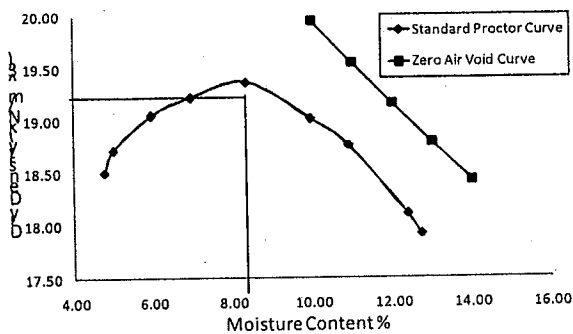


Fig. 1 Standard Proctor Curve of quarry dust

According to the proctor compaction test, the maximum dry density of the quarry dust sample was  $19.37 \text{ kN/m}^3$  and the optimum moisture content was 8.3%.

### 3.2 Determination of field dry density in each trial

- Total wet weight of quarry dust is measured before filling the container. ( $W_{wet}$ )
- Dry weight of the quarry dust is obtained by measuring the average moisture content of the sample. ( $W_{dry}$ )
- Since containers are rigid, the sectional areas are considered to be constants, so that the volume of compacted quarry dust is determined by measuring the average height of quarry dust after compaction. ( $V_{avg}$ )
- Then the field dry density can be obtained by knowing the dry weight of quarry dust and

average volume of sample after the compaction. ( $V_{dry,field}$ )

- Finally after knowing the field dry density in each trial and the maximum dry density from Standard Proctor Compaction Test, the degree of compaction can be determined in each trial.

### 3.3 Idealization and special considerations

- Containers used in experiments are having diameter and width of about 1 m, which can be idealized as individual circular and rectangular footings. (Used for shallow foundations.)
- Since the containers are made with rigid materials, it can be considered as same as the boundaries in footing excavations in ground, where the excavated surface can be considered as relatively rigid when comparing with the filling material.
- Quarry dust is filled in loose state at the beginning where no any other effort is given initially to compact quarry dust except the compaction given by poker vibrator.
- Since quarry dust is used as a filling material in sites where the ground water table is encountered in most of the time, all the experiments are conducted under saturated condition.

### 3.4 Variation of parameters

Parameters to be varied are selected after carefully reviewing the literature, where the highest priorities are given to the parameters which may highly affect the degree of compaction.

#### 3.4.1 Time of application of Poker Vibrator

While keeping other parameters as constants the time of application of poker vibrator has increased gradually in 5 s increments. I.e. 5 s, 10 s, 15 s, etc. Two experiments were conducted to find out a reasonable optimum application time of vibrator and that time period is used for other experiments.

#### 3.4.2 Shape of the containers used

The experiments were conducted in circular and rectangular shaped containers, where the dimensions of the containers are approximately equal to each other and similar to practical situations as well. The shapes and the average dimensions of the containers used, can be illustrated as follows.

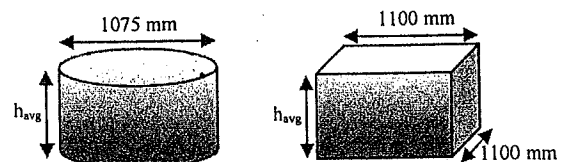


Fig. 2 Shape of the containers used

3.4.3 Distance between two points of application of Poker Vibrator (Pattern)

Several patterns were identified as more suitable to achieve higher degree of compaction in quarry dust and they were adopted to conduct the experiments.

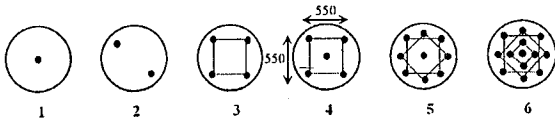


Fig. 3 Patterns used in circular container

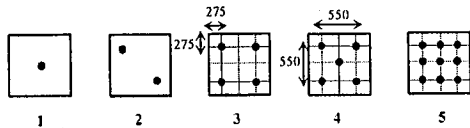


Fig. 4 Patterns used in rectangular container

\*All dimensions are in millimeters.

3.4.4 Layer thickness of quarry dust

In most practical situations quarry dust has to be filled in several layer thicknesses according to the excavation depth, level of ground water table, etc. Thus it is necessary to assess the variation of DOC by conducting the experiments for several layer thicknesses. Mainly experiments were conducted for three layer thicknesses, which are 300 mm, 450 mm and 600 mm.

4 RESULTS AND DISCUSSION

4.1 Variation of Degree of Compaction w.r.t. application time of poker vibrator

Two experiments were conducted for pattern 01 and pattern 02 in circular container with an initial layer thickness of 300 mm, to assess the effect on application time of poker vibrator.

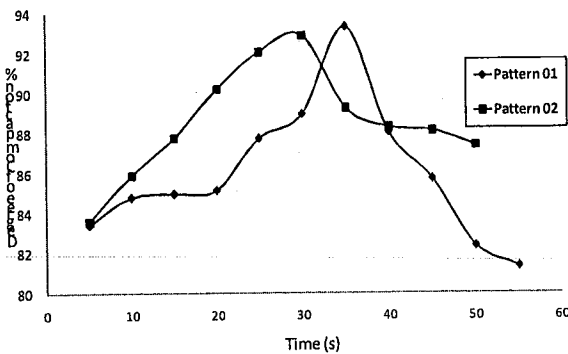


Fig. 5 Variation of DoC w.r.t time

- Both variations follow the same order where DoC is increasing w.r.t. time, up to 30s – 40s and decreasing again after reaching a peak value.

4.2 Variation of Degree of Compaction w.r.t. application pattern of poker vibrator

The variation of DoC w.r.t. application pattern was assessed by conducting series of experiments where results were plotted in several graphs, in order to compare the effect of layer thickness and shape of container.

All the experiments are conducted with an application time of 35 s per application point, which can be considered as an optimum application time as obtained from previous results. (See fig 5)

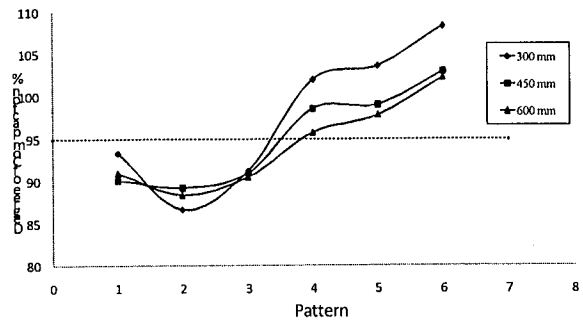


Fig. 6 Variation of DoC w.r.t. patterns for different layer thicknesses in circular container

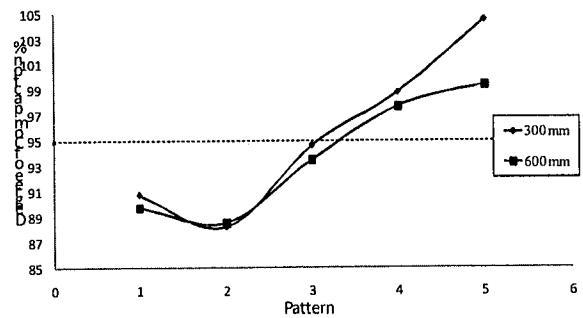


Fig. 7 Variation of DoC w.r.t. patterns for different layer thicknesses in rectangular container

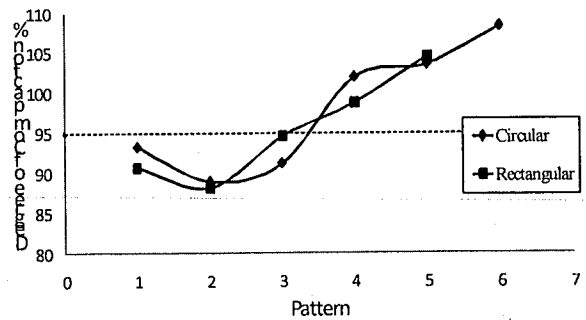


Fig. 8 Variation of DoC w.r.t. patterns in different shaped containers for 300 mm initial layer thickness

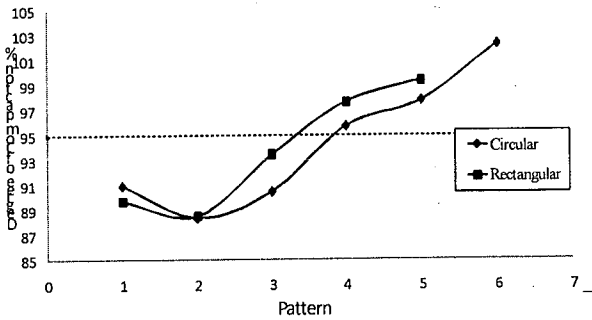


Fig. 9 Variation of DoC w.r.t. patterns in different shaped containers for 600 mm initial layer thickness

- When considering above 4 figures, it can be noticed that all the variations are following the same order, such that DoC is increasing w.r.t. pattern.
- In most cases pattern 4, 5, 6 give DoC s greater than 95% and in some cases (pattern 6) it is more than 100%.

4.3 Variation of Degree of Compaction w.r.t. layer thicknesses

Series of graphs were plotted by assessing the variation between initial layer thickness and DoC, in order to compare the effect of pattern and shape of the container.

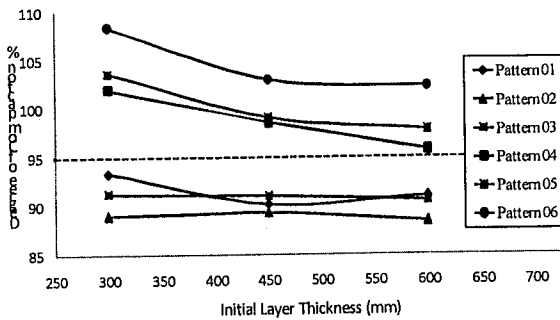


Fig. 10 Variation of DoC w.r.t. thickness for different patterns in circular container

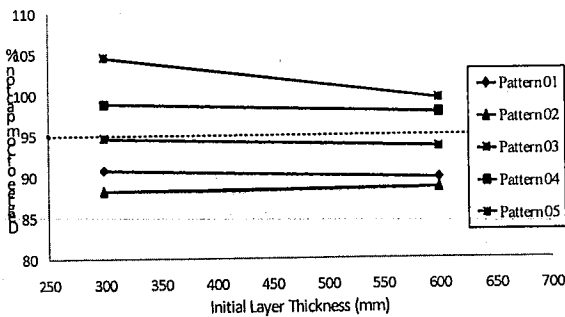


Fig. 11 Variation of DoC w.r.t. thickness for different patterns in rectangular container

- DoC s in both containers are following a same variation, such that DoC decreases with layer thickness for all patterns.
- Also in both cases DoC s are greater than 95% for pattern 4, 5 and 6.

5 CONCLUSIONS AND RECOMMENDATIONS

- The optimum time period of application of poker vibrator is around 30 s – 40 s per one point (see fig 5), otherwise material may get loosen again due to excessive vibration and it may diminish the DoC.
- DoC s in both circular and rectangular containers follow a same variation pattern (see fig 6,7).
- In most cases, application of vibrator at the middle (pattern 01) gives a relatively higher DoC when comparing with the application at corners (pattern 02 ad 03). This may happen due to availability of rigid boundary, which will hinder the vibration effect. (see fig 6,7,8,9)
- However an acceptable DoC (>95%) can be achieved with pattern 04 in most cases where the vibrator is applied at middle as well as four corners. Thus, pattern 04 can be recommended as an optimum pattern.
- In every case, it can be noticed that DoC decreases with the initial layer thickness. (see fig 10,11) However by adopting pattern 04, 05 or 06, acceptable DoC s can be achieved at once, even with a 600 mm layer thickness.

6 REFERENCE

Aziz Al-Mosawe Mosa J., Albusoda B.S. and Yaseen A.S. (2009). Bearing capacity of shallow footing on soft clay improved by compacted cement dust. Journal of Engineering. 15(04), 4417-4428.

Drnevich V., Evans A. and Prochaska A. (2007). Study of effective soil compaction control of granular soils. School of Civil Engineering, Purdue University. FHWA/IN/JTRP-2007/12.

Indraratna, B. and Chu, J. (2005) Ground Improvement – Case Histories, Elsevier, 1115p

Kumar U.A. and Biradar K.B., (2014). Soft sub grade stabilization with quarry dust-an industrial waste. International journal of research in engineering and technology. 03(08), 409-412.

Onyelowe ken C., Okafor F. O. and Nwachukwu D. G. (2012). Geophysical use of quarry dust (as admixture) as applied to soil stabilization and modification. ARPN journal of earth sciences. 1(1), 06-08.

Robert V. Whitman R.V. and Ortigosa de Pablo P. (1981). Densification of sand by vertical vibration.

Satyanarayana P.V.V, Pradeep N. and Nandhini N. (2013). A Study on the Performance of Crusher Dust In Place Of Sand and Red Soil as A Sub grade and Fill Material. IOSR Journal of Mechanical and Civil Engineering. 09(02), 53-57.